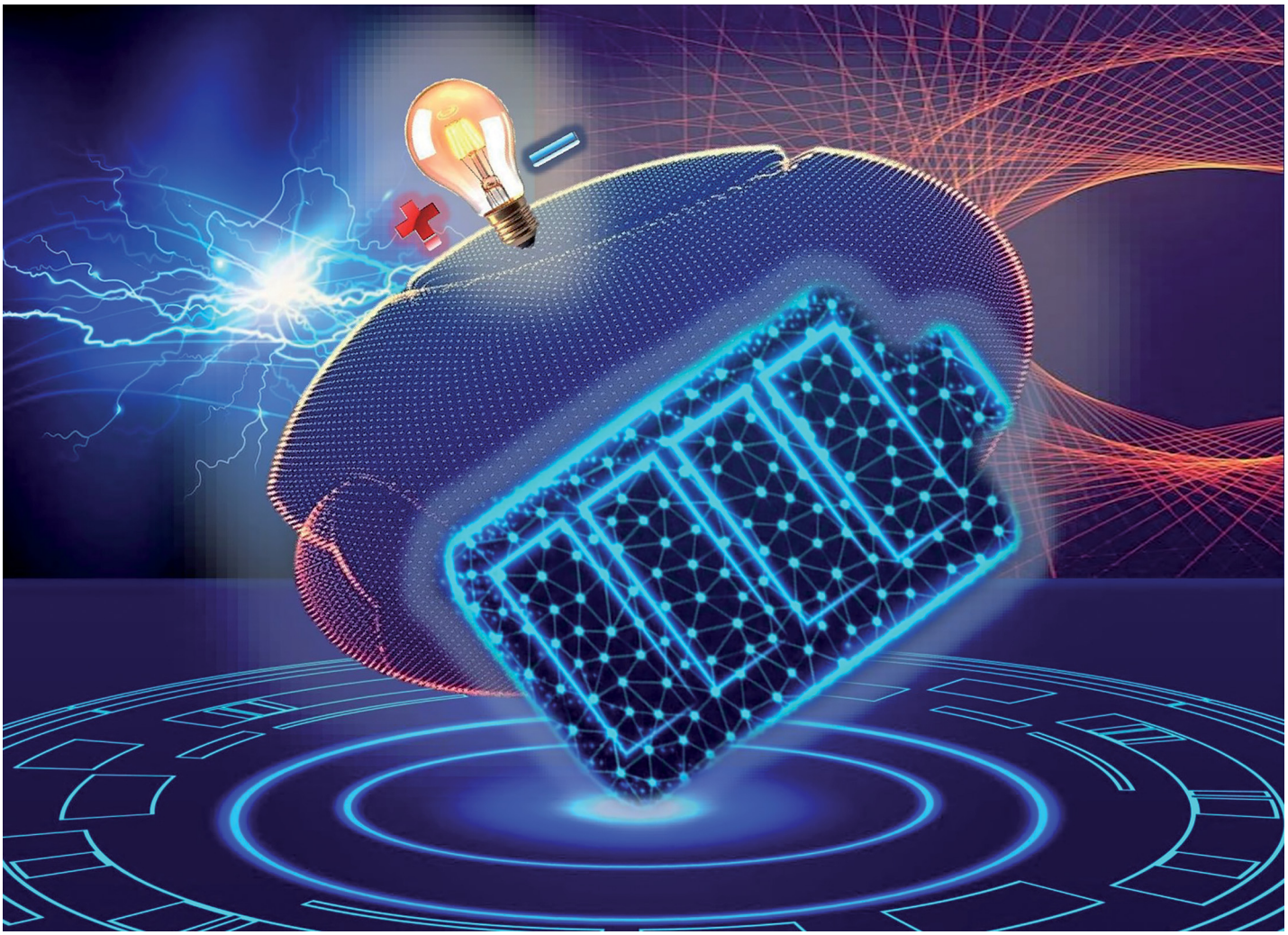

Showcasing research from Professor Chandra Sekhar Rout' laboratory, Centre for Nano and Material Sciences, Jain University, Bangalore, India

MXene–carbon based hybrid materials for supercapacitor applications

In this article authors highlight the latest progress, limitations, challenges and future perspectives of MXene–carbon based hybrid materials for supercapacitors applications. Further, synthesis methods, competitive features and applications of MXene–carbon hybrid nanocomposites for energy storage applications are discussed. This article aims to explore the practical implementation of the discussed electrode materials in the realm of supercapacitor research, offering valuable insights for future investigation into these highly promising materials.

As featured in:

See Sang Mun Jeong, Chandra Sekhar Rout *et al.*, *Energy Adv.*, 2024, **3**, 341.

ROYAL SOCIETY OF CHEMISTRY

rsc.li/energy-advances

Registered charity number: 207890

Energy Advances

ROYAL SOCIETY OF CHEMISTRY

REVIEW ARTICLE

View Article Online
View Journal | View Issue

Cite this: *Energy Adv.*, 2024, 3, 341

MXene–carbon based hybrid materials for supercapacitor applications

Pavithra Siddu N. K.,[a] Sang Mun Jeong *[b] and Chandra Sekhar Rout *[ab]

Designing hybrid materials with superior electrochemical properties has attracted tremendous interest in recent years for energy-storage applications owing to a high demand for energy sources and the depletion of fossil fuel resources. In this regard, supercapacitors have attracted considerable interest considering their excellent characteristics and superior performance. Among these material families, one group that stands out, particularly in electrochemical energy-storage applications, is 2D transition metal carbides and nitrides, commonly referred to as MXenes, alongside carbon-based materials such as activated carbon (AC), carbon nanotubes (CNTs), conducting polymers (CPs), and graphene (GO, rGO) owing to their remarkable thermal, electrical, and mechanical properties. This comprehensive review encompasses the most recent advancements in the exploration of supercapacitors based on MXene/carbon-based composites. It delves into various aspects of these composites, such as material synthesis, electrode materials, electrochemical performance, and diverse applications, offering an in-depth analysis of this field. This article seeks to explore the practical implementation of MXene/carbon-based composites in the realm of supercapacitor research, offering valuable insights into these highly promising materials for future investigations. Accordingly, a detailed literature review was carried out. Finally, the current trends, limitations, and future perspectives of MXene–carbon-based materials for supercapacitor applications are proposed.

Received 11th October 2023,
Accepted 4th January 2024

DOI: 10.1039/d3ya00502j

rsc.li/energy-advances

1. Introduction

Worldwide energy consumption has significantly increased as a result of the rapid population growth and industrialization. The demand for efficient and sustainable energy-storage systems is propelled by the depletion of fossil fuels and consequent energy

[a] *Centre for Nano and Material Sciences, Jain University, Jain Global Campus, Jakkasandra, Ramanagaram, Bangalore-562112, India. E-mail: csrout@gmail.com, r.chandrasekhar@jainuniversity.ac.in*
[b] *Department of Chemical Engineering, Chungbuk National University, Cheongju, Chungbuk 28644, Republic of Korea. E-mail: smjeong@chungbuk.ac.kr*

Pavithra Siddu N. K.

Pavithra Siddu N. K. completed her bachelor's degree from K. L. E. Society's S. Nijalingappa College, affiliated with Bangalore University, Bangalore, Karnataka, India (2019). Later, she moved to M. S. Ramaiah University of Applied Science, Karnataka, India, to pursue a master's in industrial chemistry (2020–2022). Currently, she is a doctoral student in nanotechnology at CNMS, Jain University, working under Prof. Chandra Sekhar Rout, with his research focused on the energy and environmental applications of 2D nanomaterials.

Sang Mun Jeong

Sang Mun Jeong is a Professor at the Department of Chemical Engineering at Chungbuk National University, South Korea, a leading Regional Leading Research Center (RLRC) for developing next-generation battery materials funded by the National Research Foundation of Korea, and a director of Korea Institute of Chemical Engineers. Also, he was a Dean of the research affairs of Chungbuk National University (2021–2023). His research focuses on energy-related materials and processes based on chemical and electrochemical engineering to develop efficient, clean, and renewable future energy solutions.

crisis, thus driving the search for environment-friendly and high-performance energy-storage devices.[1–3] More advanced and effective storage methods are required for the storage of energy produced by renewable resources. In this view, supercapacitors and batteries are the most widely studied candidates for energy storage. In devices that have batteries with high massic energy, capacitance is inversely proportional to electrode separation and directly proportional to the electrode area, and hence, supercapacitors are excellent energy-storage electrochemical devices with less input resistance, high power density, long durability, expeditious charge discharge, and eco-friendly nature. Consequently, supercapacitors have gained more popularity compared to batteries.[4,5] Supercapacitors are also known as ultracapacitors. Based on their mechanism of energy storage, they are classified into two unique categories: electrochemical double-layer capacitors (EDLCs) and pseudo capacitors.[6–8] The primary focus of several ongoing studies is to explore suitable electrode materials for supercapacitors, aiming to enhance both high specific energy and power while significantly prolonging their cycling life. Among the studied materials, MXenes, a class of two-dimensional (2D) materials, have been extensively reported by Gogotsi *et al.* in 2011[9–11] to have exceptional hydrophilicity and metallic conductivity. This composition is commonly represented as $M_{n+1}AX_n$, where M denotes a transition metal, A signifies a group of elements from IIA or IIIA, and X symbolizes nitrogen or carbon. MAX phases can also be referred to as A layer-bonded layered 2D transition metal nitride and carbide phases. The chemical formula of an etched MXene is represented as $M_{n+1}X_nT_x$, where T stands for surface functional groups (OH, F, and O). MXenes perform admirably in practically all electrolyte media. It has been reported that the electrochemical-charge-storage capability is remarkable in MXene-based electrodes in supercapacitors owing to several influential factors (Fig. 1).

The energy-storage capacity of individual MXene electrodes is, however, limited by some challenges, such as agglomeration, low energy-storage density, and the tendency of the multilayer structure to undergo spontaneous collapse during initial cycles. To overcome this issue, MXenes can be combined with other one-dimensional (1D) carbon-based materials in a synergistic manner to further enhance their energy-storage capabilities.[12] Where sp^2 hybridized carbon atoms are arranged in a hexagonal lattice in carbon materials. These can have several uses in various fields, including energy-storage devices, field-effect transistors, sensors, and other gadgets, because of their remarkable characteristics (thin, transparent, and flexible). The significance of MXenes and an overview of several carbon-based electrode materials are discussed herein. The key methods to improve the energy-storage performance by altering the material morphology and surface engineering/functionalization are thus described. Also listed herein are the difficulties and prospects for achieving high structural excellence and exceptional capacitance performance. The significance of carbon-based materials, their synthesis, crystal structure, the evolution of supercapacitors, and recent advancements and

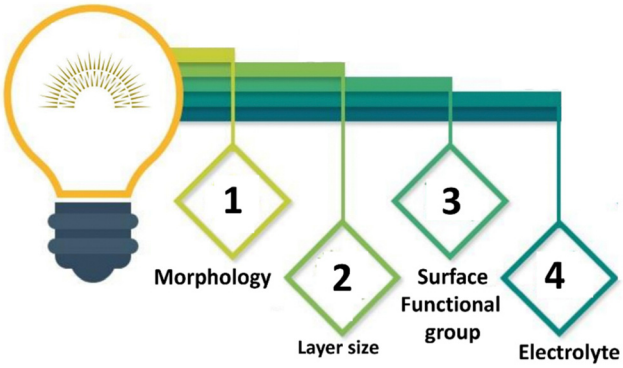

Fig. 1 Several influential factors that can affect the performance of MXene-based electrodes in supercapacitors.

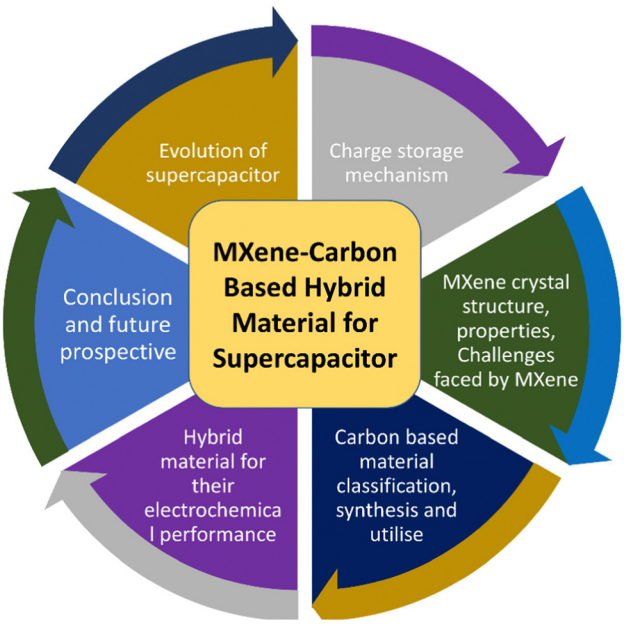

Fig. 2 Detailed summary of the content of the review.

Chandra Sekhar Rout

Prof. Chandra Sekhar Rout is a full professor at the CNMS, Jain University, India. Before joining CNMS, he was a DST-Ramanujan Fellow at IIT Bhubaneswar, India (2013–2017). He did his PhD at JNCASR, Bangalore (2008), followed by postdoctoral research at NUS, Purdue University, and UNIST. His research is focused on the applications of 2D layered materials for different devices. He has authored more than 200 research papers and 6 books. His h-index is 55, with >13 000 total citations. A Stanford study ranked him in the top 2% of scientists in 2020–2022.

applications towards effective supercapacitor electrode materials are all outlined in this paper. Fig. 2 provides a schematic illustration that outlines the content of the present review in a concise manner.

2. Evolution of supercapacitors

The energy source of choice for daily instruments that require day-long power is batteries, while supercapacitors are utilized for quicker power charging and discharge. Supercapacitors (SCs) are also called ultracapacitors or electrochemical capacitors;[13] wherein supercapacitors have an energy-storage capacity per unit of mass or surface that is comparatively lower, hence they utilise materials with a huge surface area as electrodes than thin dielectric fluids to achieve capacitors with numerous orders of magnitude higher capacitance than natural capacitors. Incorporating materials into these can allow supercapacitors to achieve larger energy densities while maintaining higher power densities, which is a hallmark characteristic feature of normal capacitors.

Where used in a normal capacitor, double conducting electrodes are separated by a dielectric material, and then upon applying voltage to the capacitor, opposing charges accumulate on the surfaces of both electrodes. The dielectric of a capacitor plays a crucial role in separating the charges and generating an electric field, facilitating the storage of energy. The ratio of the stored charge (Q) to the voltage that is being applied (V) is known as the capacitance (C):

$$C = Q/V \text{ (Farad)} \quad (1)$$

The capacitance (C) of a conventional capacitor is directly proportional to the electrodes surface area (A) and inversely proportional to their separation distance (D):

$$C = (\in_0 \in_r A)/D \text{ (Farad)} \quad (2)$$

where, $\in_r r$ is the relative permittivity of the insulator separating the anode and cathode and influences the system's performance, and $\in_0$ is the dielectric free space permittivity constant. The energy and power density of a capacitor are significant characteristics that can be evaluated in terms of the unit volume or quantity per unit mass. The capacity a capacitor can store, denoted as E, is directly proportional to its capacitance and the voltage squared:

$$E = (CV^2)/2 \ (W \text{ or } J) \quad (3)$$

In SCs various charge-storage characteristics are caused by the electrochemical reactions inside of them. Electric double-layer capacitors (EDLCs) or supercapacitors, store electrical charges by the adsorption of electrolyte ions on the electrode materials. High power causes potential changes that can make the reaction occur more quickly. There are numerous characterization techniques for achieving double-layer capacitance, including cyclic voltammograms with a rectangular shape and time-dependent linear potential change with constant current. Reversible reduction and oxidation events that take place at or close to the surface of a suitable electrode material lead to the structures of an EDLC, but the reactions also lead to superior charge storage. This technique of pseudocapacitance illustrates the capacitive nature of energy storage. Pseudocapacitors have higher power storage densities, cycle lifetimes, and energy-storage densities. Metal oxides, like Co_3O_4, and RuO_2, other nitrides, and carbides also show pseudocapacitance behaviours.

2.1. Types of supercapacitors

Supercapacitors can be categorized into three categories: hybrid capacitors,[14] electrochemical double-layer capacitors,[15] and false- or pseudocapacitors.[16] These three classes serve as an example of their typical charge-storage techniques. Electrode and electrolyte charge transfer play important roles, such as in faradaic processes, like redox reactions. Surprisingly, a non-faradaic technique does not use redox chemical reactions,[17] and surface charges are spread physically, without considering chemical processes.

2.1.1. Electric double-layer capacitance. In an EDLC supercapacitor, charges are separated by the Helmholtz double-layer interface among the conductive surface of the electrode and the electrolyte to store electrostatic energy.[18]

The mechanism of charge storage in EDLCs depends on the electrostatic adsorption of the electrolytic ions on the electrode surface. Therefore, the way to get high capacitance for EDLCs is by using an electrode material with a more efficient accessible surface area in addition to its good electronic conductivity, *i.e.* selecting the electrode material is a critical step to improve the behaviour of SCs. A double layer's static charge-separation distance is in the order of nanometres. Through the process of charging the double layer and exploiting conducting electronic electrodes, nanostructured carbon-based materials with a great specific surface area (SSA) is a significant factor for generating high capacitance. Carbon-based materials include graphene and its derivatives activated carbon (AC), carbon nanotubes, carbon nanohorns, carbon fibers, carbon cloth, and porous carbons. The ideal voltage linearly drops during discharge in EDLC capacitors.[19] The square of the voltage affects how much energy the ideal EDLC can store. In EDLC electrodes, carbon and its derivatives have been tested and widely used.[20] The material is characterized by its good electrochemical stability, high electrical conductivity, and highly accessible surface area, besides its low cost and ease of processing. Over the last years, porous electrode structures have attracted considerable attention, providing very high SSAs and well-defined pathways for electrolyte access. The capacitance of EDLCs is analogous to a conventional capacitor and can be described as follows,

$$C = \in_r \in_0 A/d$$

where $\in_r$ is the relative dielectric constant in the double layer, $\in_0$ is the permittivity of free space, and d represents the effective thickness of a double-layer with the surface area A.

As a result of the electrostatic charge-storage mechanism, including no faradaic reaction at the EDLC electrodes surface, EDLCs allow very rapid energy uptake and delivery, *i.e.* they exhibit better power performance than batteries. Hence, highly reversible charging/discharging and excellent cycling life are

achievable for EDLCs, whereas batteries can continue for a few thousand cycles at best. Besides, the solvent of the electrolyte is not involved in the charge-storage mechanism, unlike in lithium-ion batteries where it contributes to the solid–electrolyte interphase. High-capacitance EDLCs can also achieved by increasing the electrode surface area, which can be additionally increased by using a porous structure. EDLCs typically charge storage (up to 0.25 atomic surface electrons) by surface absorption, which allows them to discharge higher power densities, and achieve longer life cycles, but with lower energy densities.

2.1.2. Pseudocapacitors. In the most highly advanced pseudocapacitors,[21] the transfer of electrons for electrochemical energy storage occurs through redox reactions at the surface, involving the passage of charge across the double layer by redox reactions at the surface with the specific adsorption of electrolytic ions, the intercalation or diffusion of atoms in the electro-adsorption process or layer, or deposition of metal or hydrogen in the lattice sites. These processes facilitate a reversible faradaic charge transfer within an impressive ratio of 2.7 surface electrons per atom. Importantly, the electrical response of a pseudocapacitive material is ideally the same as that of a double-layer capacitor. The pseudocapacitors energy density is typically greater than that of EDLCs. The major materials used in pseudocapacitors are conducting polymers and metal oxides (nitrides, sulphides, and oxyhydrides). faradaic processes occurring together with EDL-charge-storage increase the specific capacitance of an electrode. The capacitance of a pseudocapacitor can be 10–100 times higher than that of an EDLC. Nevertheless, the power performance of a pseudocapacitor is usually lower than that of an EDLC, due to the slower faradaic processes involved. Electrodes exhibiting pseudocapacitance are more prone to swelling and shrinking in charge/discharge cycling, which can lead to poor mechanical stability and a low cycle life.

2.2. Mechanisms for storing charge

The operation of SCs generally involves three main charge-storage mechanisms (Fig. 3): (1) One involving the electric double layer in an EDLC. Here, the dual charged layers that develop at the interfaces of electrolyte/electrode are identified as the electrical double layer (EDL).[22] Early EDLs were sometimes referred to as Helmholtz double-layers, because they were typically associated with Helmholtz energy. The Gouy–Chapman–Stern and Gouy–Chapman models define the specific structures of EDLs. Activated carbon with a greater surface area is often used as the medium in EDLCs. Due to their larger surface area, EDLCs can store more electricity that is measured in Farads, while in conventional electrolytic and dielectric capacitors it is frequently expressed in terms of picofarads and microfarads. (2) Another involving a highly reversible surface reduction and oxidation system integrated into the supercapacitor. This system was developed by Trasatti,

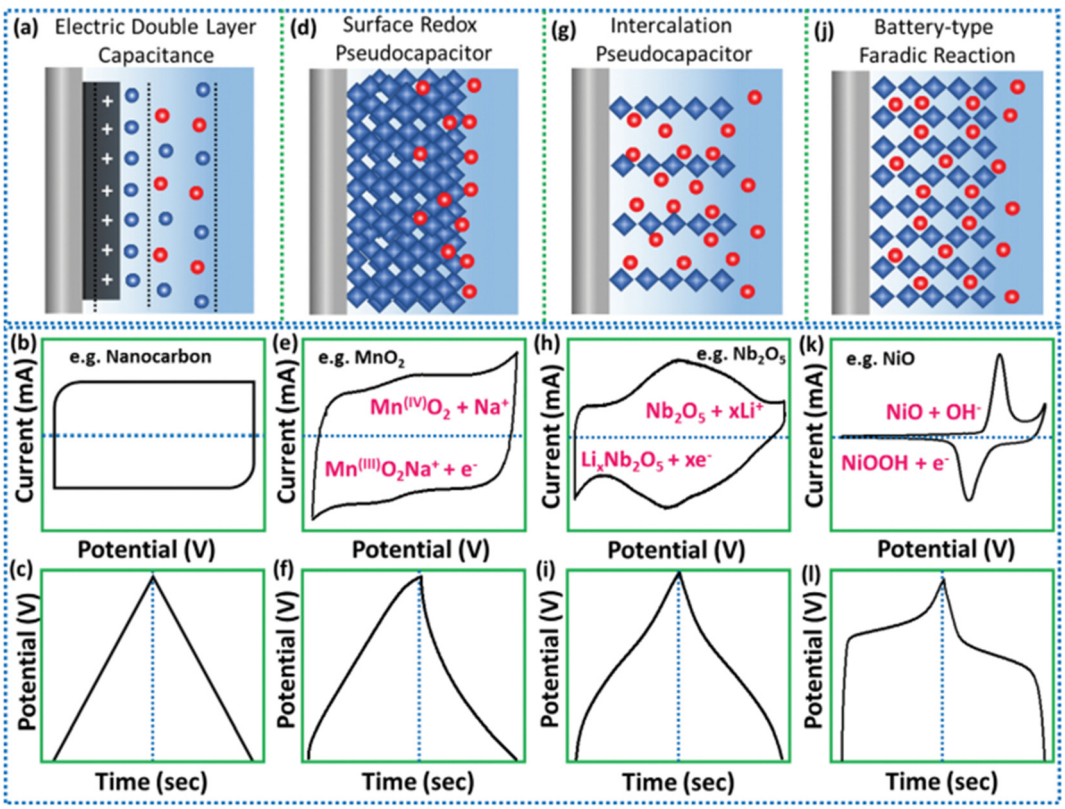

Fig. 3 Electrochemical signatures of energy-storage techniques are shown schematically, together with their representative CV and CD curve shapes: (a)–(c) EDLC, (d)–(f) surface oxidation reduction capacitance, (g)–(i) capacitance intercalation, and (j)–(l) faradaic battery-type. Reprinted with permission from ref. 25. Copyright John Wiley and Sons, 2020.

and is associated with a large reversible redox surface reaction, facilitating an incomplete transfer of charge among the electrolyte and the electrode.[23] Although being charged, metal oxide electrode materials that are active in both reduction and oxidation are reduced to decrease their oxidation states besides absorbing electrolytic cations. The reverse of this action occurs during discharge. Pseudocapacitors between the electrode and electrolyte feature an incomplete movement of faradaic charge at the junction, in contrast to EDLCs, which allows storing electrical charges statically without any faradaic charge transfer. (3) A process involving the rapid transport of electrolytic ions and an intercalation process,[24] both of which take place in pseudocapacitors. Electrolytic ions travel through the electrode materials during discharging and discharging in the pseudocapacitive intercalation process, which is diffusion controlled. These share two great characteristics (1) quick reversibility during charging and discharging and a (2) charge-dependant potential.

2.2.1. Hybrid supercapacitors overall capacity for charge storage. In practice, a supercapacitor's ability to store charge is improved by a mixture of numerous such charge-storage techniques.[26–28] For instance, the development of EDLs regulates the charge storage of EDLCs based on AC, but oxidizing groups on the surface of the AC may also activate some surface-based reduction and oxidation actions.[29] Even yet, asymmetric or hybrid capacitors that include different EDLC and pseudocapacitor electrodes have been reported to show improved energy performance while retaining their internal greater power delivery properties.[30]

2.3. Performance evaluation of supercapacitors

Three essential characteristics—equivalent series resistance (RES), total cell capacitance (CT), and voltage of operation (VO)—are repeatedly employed to gauge the performance of supercapacitors, allowing designers and manufacturers to make products that are suitable for commercial markets while also analysing their performance in terms of power and energy. A brief glance at the complex relationships between the various demands for specific recital requirements and their interrelationships, the majority aspects required, and the proper testing methods shows that a broad variety of significant features are required to produce supercapacitors for different applications.[31] The schematic diagram in Fig. 4 shows these demands, using a variety of colour schemes to highlight the different aspects, whereby the three vital parameters are highlighted in blue, followed by the power and energy density aspects in orange, the time stability and cycling stability requirements in dark blue, and additional important characters in yellow, as well as the appropriate system of testing in white. Be aware that the chart does not include all the components or fully describe the intricate relationships between them; it is primarily intended as an illustration. For instance, the comprehensive influence of the electrolyte materials on the specific capacitance and mechanism for evaluating V_o are not fully described. A wide range of performance measurements, test procedures, influencing factors, as depicted in the schematic depiction, and the complex interconnections between them are provided. Also, note the standards have been established after several experiments.

3. Evolution of MXenes

3.1. MXenes (structures, surface terminations, and synthesis)

A multitude of applications, such as energy conversion, medicinal devices, and energy storage, heavily rely on 2D

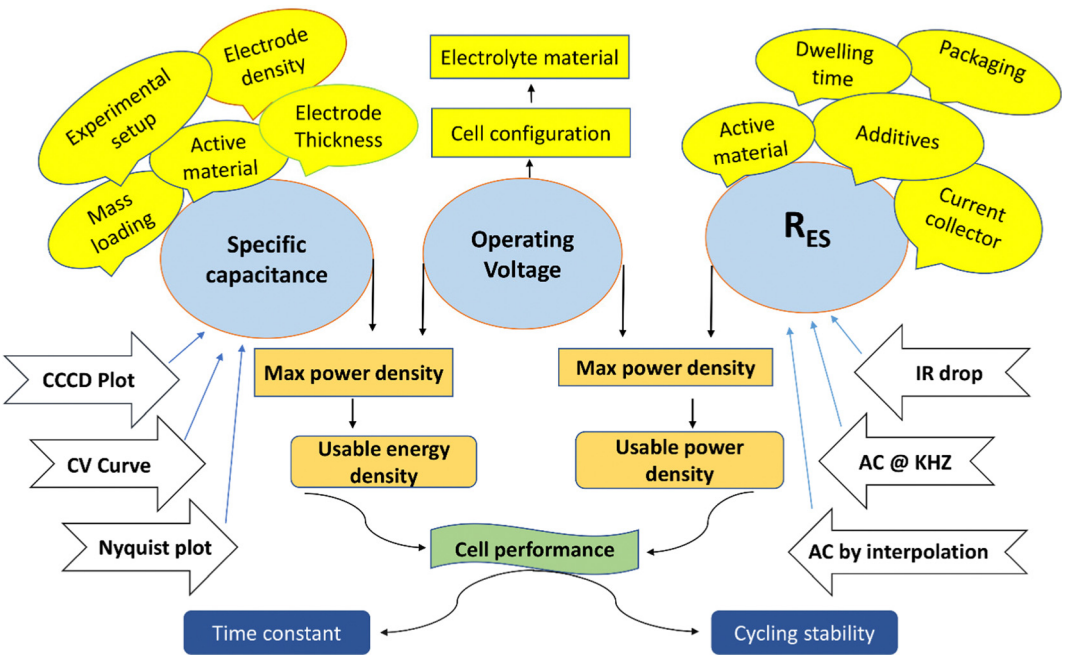

Fig. 4 Schematic showing the significant performance measures, testing methods, and influencing aspects for the evaluation of SCs.

nanomaterials.[32] They are superior to their bulk counterparts in terms of mechanical, physical, chemical, optical, and electrical properties, and consequently, 2D materials have attracted a lot of in a diversity of scientific areas, including chemistry, material science, and nanotechnology. Beyond the discovery of graphene, various layered precursor materials have been exfoliated over the past 17 years to produce various 2D nanomaterials, including black phosphorus (BP),[33] transition metal oxides (TMOs),[34] layered double hydroxides (LDHs),[35] transition metal dichalcogenides (TMDs),[36] graphitic carbon nitride (g-C_3N_4),[37] hexagonal boron nitride (hBN),[38] and metal phosphorus trichalcogenides (MPS_3).[39] In addition to the above instances of layered materials, which have a wide range of applications due to their adaptable structure and composition, Gogotsi *et al.* published the first successful investigation to produce 2D transition metal carbides, carbonitrides, and nitrides, termed as ''MXene'', in 2011, which could be succinctly epitomized by the formula $M_{n+1}X_n$. By using HF solution etching process and selectively extracting the 'A' layer from the MAX phase (Ti_3AlC_2), the first MXene (Ti_3C_2) was produced.[40] Barsoum introduced the MAX phase in 2000 and gave it the chemical formula $M_{n+1}AX_n$, where M represents an early transition metal (such as Ti, Cr, Sc, Mn, V, Zr Mo, Hf, Nb, Hf, Ta, or W), ''A'' is frequently selected from the IIIA or IVA group elements (*e.g.* elements from groups 13–16, like P, Si, S, Ge, Ga, Al, In, As, Tl, Sn, and Pb), and X can be either carbon or nitrogen or a combination of both MXene formulations and layered solid MAX phase, with n = 1, 2, or 3. The conventional name of 2D MXene Ti_3C_2 is ''$Ti_3C_2T_x$'', where ''T'' stands for a number of corresponding termination groups gracing its surface, such as hydroxyl, oxygen, and fluorine groups. Chemical etching of the atomic layer ''A'' produced the first MXene. In a number of articles, Anasori *et al.* presented every MAX phase ever discovered at that time as well as every different MXene they had so far synthesized.[41] Other kinds of MXene have since been synthesized using the same processes as the original MXene. The nomenclature trend also follows the preceding pattern. Some examples of MXene materials that are frequently used in research disciplines, including in energy conversion and energy storage, include $Ti_4N_3T_x$, Ti_2CT_x, $Zr_3C_2T_x$, $V_4C_3T_x$, V_2CT_x, Cr_2CT_x, $Ti_3C_2T_x$, $Ta_4C_3T_x$, and $Nb_4C_3T_x$. The following reactions below illustrate the most typical method of etching by using hydrofluoric acid (HF) selectively while functionalizing the MAX phase (Fig. 5 and 6), where eqn (1) depicts the transition from the MAX phase to the $M_{n+1}X_n$ phase as a result of the removal of the ''A'' atom. Further, according to eqn (2) and (3), the strategic incorporation of OH and F elements into $M_{n+1}X_n$ MXene. respectively, produces $M_{n+1}X_nT_x$ MXenes. As was already mentioned, the surface functionalities are defined by the term T.[42]

$$M_{n+1}AX_n + 3HF \rightarrow AF_3 + 3/2H_2 + M_{n+1}X_n \quad (4)$$

$$M_{n+1}X_n + 2H_2O \rightarrow M_{n+1}X_n(OH)_2 + H \quad (5)$$

$$M_{n+1}X_n + 2HF \rightarrow M_{n+1}X_nF_2 + H_2 \quad (6)$$

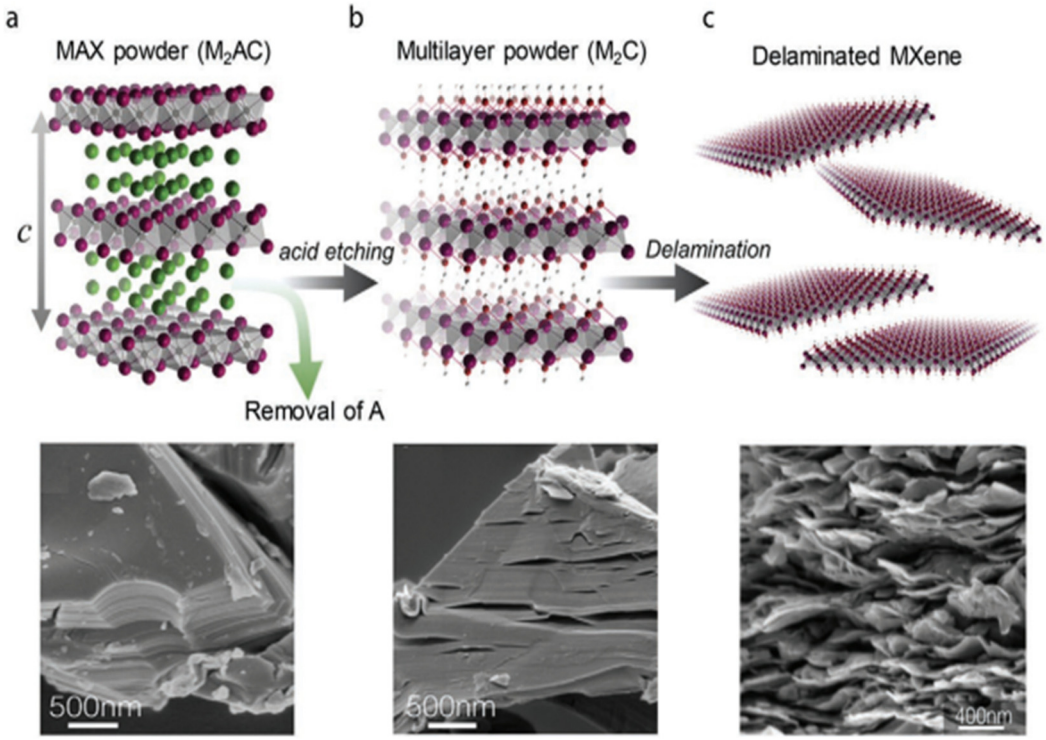

Fig. 5 Top-down etching routes for the synthesis of MXene flakes. Ordinarily, the ''A'' atomic layer in (a) HF, bifluoride-based etchants (NH_4HF_2), or HF-containing salt can be used to selectively remove stacked MAX phase powders, resulting in (b) MXene particles with several layers. Following sonication, further metal cation intercalation, DMSO, and TBAOH produce (c) delaminated single-flake MXene suspensions. Top row. Reprinted with permission from ref. 44. Copyright 2020, John Wiley and Sons.

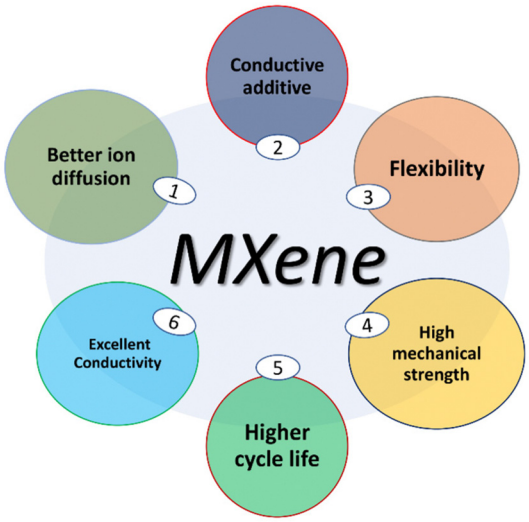

Fig. 6 Application-specific MXene properties for supercapacitors.

In addition to the primary method of using HF to remove "A" atomic layers, there are additional etching methods to produce MXenes from the MAX phase, such as direct intercalation, modulation of the layer spacing, synthesizing the $M_{n+1}X_n$ phase without the surface functionalities using chemical vapour deposition (CVD),[43] and the innovative *in situ* separation of fluoride to a cation, each offering a diverse avenue for material creation and modification.

The phonon dispersion and cohesive energy (E_{coh}) spectra can be used to study the thermodynamic stability of MXene materials. The surface functional groups and the specific metal featured within the MXene structure both affect the E_{coh} values. According to Zhang *et al.*, raising the atomic number of the metal ion increases the E_{coh} value. When the surface termination groups are taken into consideration, the E_{coh} changes in the following order: (=O) > (F) > (O) > (F) > (O–H). The placement of the functional groups in relation to the diverse metal ions in the structure of MXene, along with the type of surface terminations and metal ions, yields a panorama of fluctuating E_{coh} values for MXene functionalized with different geometries.[45] As such, the electrochemical characteristics of the MXenes can be enhanced by regulating the surface terminations. The hydrophilicity of MXene results from oxygen terminations (such as O and O–H), which enhance the ion interactions with the electrolyte and enhance the pseudocapacitive behaviour. In contrast, terminations containing F result in decreased surface-active sites, which prevent ion transfer in the electrolyte and reduce electrical conductivity. To synthesize MXenes, a fluoride-free etching technique can also be used. According to reports, the electrochemical performance of MXenes obtained using the F-free etching procedure is limited, possibly as a result of the lack of quality of the F-free etching. Many processing methods, such as Meyer rod-coating, spray- or spin-coating, writing, printing, and stamping, can be used to apply the exfoliated MXene that results from these methods.[46] The primary reported MXene (Ti_3C_2) showed a unique combination of good optical characteristics, highly accessible surface area, impressive metallic conductivity of around 9880 S cm^{-1}, large interlayer spacing, and outstanding thermal stability.[47] The general properties of MXenes are shown in the schematic representation in Fig. 6. Moreover, MXenes have demonstrated a great degree of mechanical, chemical stability, and changeable surface state. MXenes have provided a higher specific capacitance when compared with other compounds studied. For instance, films made of $Ti_3C_2T_x$ had a volumetric capacitance greater than 300 F cm^{-3}. Given their diverse properties, MXenes are widely used in numerous applications, like energy storage, including flexible batteries,[48,49] flexible-micro supercapacitors,[50] nanogenerators, and sensors.[51]

3.2. Challenges faced by MXenes

Irrespective of the excellent outcomes produced by using MXene hybrids in devices for energy storage, the implementation of MXenes into different kinds of batteries and supercapacitors is restricted by a number of challenges. For instance, it can be difficult to achieve a compromise between the mechanical characteristics of MXenes, such as their inherent inclination to face-to-face restack and random aggregation, strength, plasticity, and durability, and the electrochemical qualities in terms of flexible SCs (Fig. 7). To date, several approaches have been used to deal with the restacking difficulty, most notably the introduction of additional nanomaterials. Moreover, stacking the MXenes layers results in a significant vertical ionic diffusion resistance, which eliminates the MXenes material's rate capacity at high current density values.

Another issue that needs to be considered is the oxidation of MXenes. The harsh chemical etching procedure, which is thought to be an active aspect for the oxidation reaction of MXenes, causes flaws on the surface of the MXenes or at the edge of the flakes. As a result, the highly crystalline MXenes can degrade into TMOs, like TiO_2 and amorphous carbon, when exposed to water and/or oxygen. Suppressing the dissolved oxygen is the first step that might be taken to prevent this as the substance needs to be stored before use. This could be done

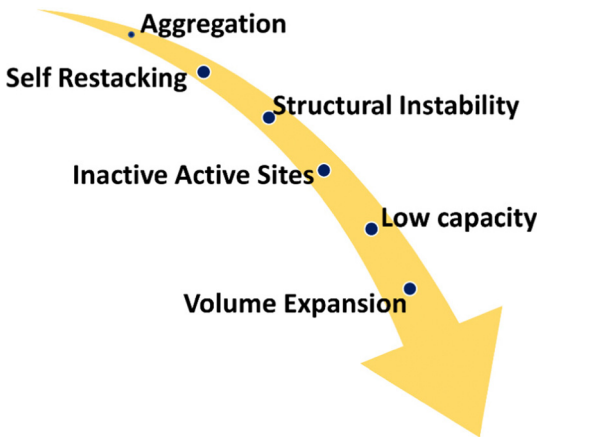

Fig. 7 Schematic showing some disadvantages of 2D materials.

by storing the solution in argon-sealed containers. Purging dry nitrogen throughout the synthesis process is a helpful approach to eliminate the dissolved oxygen in order to inhibit MXene oxidation. The temperature, content, and pH of the aq. dispersions are just a few of the parameters that must be controlled in order to provide a favourable environment for the storage of MXenes while maintaining a lower temperature to slow the rate of oxidation. Thus, it is necessary to address the issues related to the aggregation of the produced MXenes and the storage at sub-zero temperatures. Given that MXene oxidation tends to start at the edge active sites, using polymers to create MXene–polymer based composites is extremely advantageous to improve the stability of the MXenes. For instance, polar polymers with charged nitrogen ends showed a strong propensity to interact with the $Ti_3C_2T_x$ layers, increasing the interlayer gap. Physical vapour deposition and atomic layer deposition have been introduced as suitable methods to reduce the oxidation of MXenes, leading to improvements in their chemical stability in aqueous electrolytes, among other approaches to deal with the oxidation issue. Approaches to regulate the interaction of exfoliated MXene nanosheets with various solvents and to reduce the production cost without compromising the quality of the MXenes should be given more thought. Also, as exposure to MXenes may have harmful effects on the respiratory system, skin, and digestive track, comprehensive effort is also required to address the environmental hazards of MXenes.[52]

In order to reduce the use of a needlessly high HF concentration, it is also crucial to consider the risk evaluations of the HF-based etching technique and replace it with alternate protocols. *In situ* HF production from salt based-HF, such as $(NH_4)HF_2$ or fluoride salts, such as LiF, can be an alternate method for synthesizing HF-containing etchants. Also, new appropriate encapsulating techniques would be extremely helpful in the case of MXenes with a high rate of oxidation to increase the stability and lifetime of the associated devices. Also, it is important to look at how the structural features of MXenes affect their ability to store charges and behave electrochemically.[53,54] In this regard, factors like the basal spacing and surface chemistry can have a significant impact. Also, the accessibility and use of surfaces for electrochemical energy storage are severely constrained by MXene's inherent inclination to face-to-face restack and random aggregation, which is a problem shared by all other 2D materials. To date, several approaches have been reported to deal with the restacking difficulty, most notably the introduction of additional nanomaterials.[55]

Despite the difficulties highlighted, MXene materials have a bright future ahead of them because of their special features and the advancements made as a consequence of extensive study and labour in various sectors, including environmental science, biomedicine, environmental science, catalysis, energy storage, and energy conversion. However, significant efforts and research are still needed to better understand the mechanism of energy storage in MXene nanomaterials to enable them to achieve superior performances, and also to provide effective approaches to construct MXene-based supercapacitors and battery devices.[55]

4. Carbon-based materials for SCs

Carbon-based materials have demonstrated remarkable adaptability. Since they can chemically combine with other carbon-based materials and a variety of different elements to generate potent covalent bonds, they can consequently display many great qualities, like strong strength, high density, and high hardness.[56–61] The development of carbon-based materials has demonstrated numerous benefits for a variety of structural types, enabling the manufacture of numerous materials with various uses. Herein our focus is on carbon-based materials that have demonstrated promise in a range of applications intended to address the world's present energy and environmental concerns. Recent research suggests that graphene-based materials and carbon nanotubes (CNTs) exhibit vastly favourable results for many of the environmental problems that we presently face and that will become much more serious in the upcoming future if we do not prioritise the research and development of new technologies to reduce and even overcome the current serious environmental issues, including global warming and pollution from burning fossil fuels.

Some nanoparticles that are entirely composed of carbon and are referred to as carbon-based nanoparticles are schematically illustrated in Fig. 8. They can be divided into fullerenes, graphene, carbon nanotubes, carbon nanofibers, and carbon black, as well as the frequently nanoscale activated carbon in zero size.

4.1. Carbon nanotubes (CNT)

CNTs are nanotubes made of graphene nanofoils with a carbon atom like honeycomb lattice that are wound into hollow cylinders. Single-layer CNTs have a diameter as small as 0.7 nm, while multi-layered CNTs have a diameter of 100 nm. The nanotube lengths range from a few micrometres to numerous millimetres. Either a hollow end or a half fullerene molecule can close the ends. CNTs exhibit exceptional thermal, electrical, mechanical, and surface-to-weight ratios as well as enormous surface areas and high storage capacities.

4.2. Graphene

Carbon exists in various allotropes, including graphene. In graphene, the carbon atoms are organized into a hexagonal honeycomb lattice in a 2D planar surface. Typically, a graphene sheet is about 1 nm thick. Graphene has a greater intersheet van der Waals force of attraction. Its substantial surface area, micro porosity, and high electrical conductivity are the major qualities that make graphene materials viable contenders for energy-storage applications.

4.3. Carbon nanofiber (CNFs)

Carbon nanofiber, or CNFs, are made from similar graphene nanofoils as CNT but are twisted into a cone- or cup-shaped

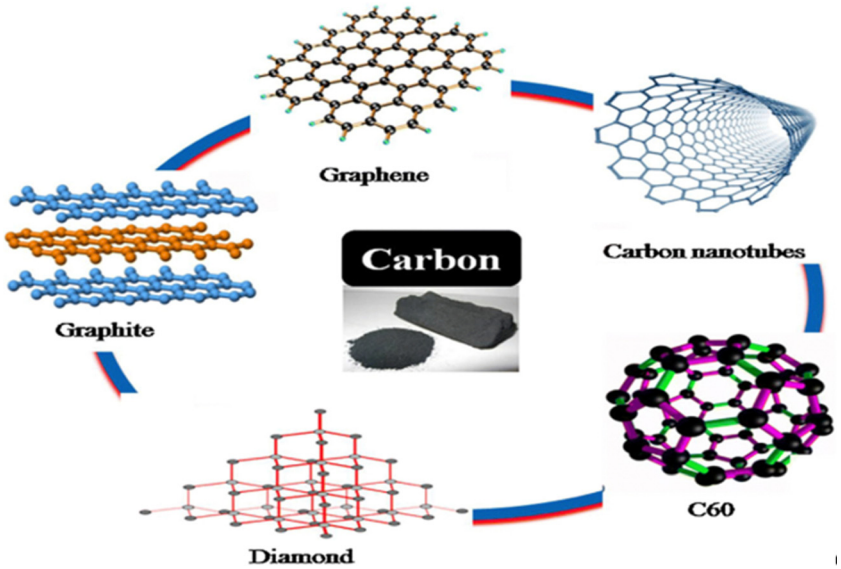

Fig. 8 Polymorphs of nano-carbon-based materials. Reprinted with permission from ref. 62. Copyright 2018, Elsevier.

structure as opposed to a conventional cylindrical tube. They offer excellent mechanical, thermal, electrical, and frequency shielding qualities.

4.4. Carbon black (CB)

CB is a carbon-based amorphous material with diameters ranging from 70 to 20 nm, that is often sphere-shaped. In order to produce agglomerates, which are about 500 nm in size, the particles' contact is so intense that they become linked together. Consequently, CB is extremely strong, electrically conductive, and surface-area wise, it can resist UV deterioration.

4.5. Fullerenes

Fullerenes (C_{60}) are spherical-shaped carbon molecules comprised of carbon atoms bound together by sp^2 hybridization with single and double bonds to form a closed mesh-like structure. With dimensions up to 8.2 nm for a single layer and 4 to 36 nm for multi-layered fullerenes, the spherical structure is made up of roughly 28 to 1500 carbon atoms. Since their discovery in 1985, they have received a lot of interest due to their chemical and thermal stability. The common properties of fullerenes allow them to act as a semiconductor, conductor, superconductor and they transmit light based on intensity. The employment of these materials in energy-storage systems is made possible by their remarkable conductivity.

4.6. Synthesis of nanomaterials

The techniques used to synthesize the nanoparticles can be categorized as either bottom-up or top-down techniques.[63–70] Atoms, clusters, and nanoparticles are built up in a bottom-up or constructive manner. The most popular bottom-up techniques for producing nanoparticles include sol–gel, spinning, chemical vapour deposition (CVD), pyrolysis, and biosynthesis. Reducing a bulk substance to the nanometre-scale particles is known as a top-down or destructive approach. A few of the most popular techniques for creating nanoparticles are mechanical milling, nanolithography, laser ablation, sputtering, and thermal breakdown (Fig. 9).

4.6.1. Bottom-up methods

4.6.1.1. Biosynthesis. In order to create nontoxic, biodegradable nanoparticles, a green and environmentally friendly method is often used called biosynthesis. Instead of using conventional chemicals for bioreduction and capping, biosynthesis creates nanoparticles using precursors and microorganisms, like bacteria, fungi, or plant extracts. The biosynthesized nanoparticles are special and upgraded in ways that make them useful in biomedical applications.

4.6.1.2. Chemical vapour deposition (CVD). The deposition of a thin film of gaseous reactants onto a substrate is known as chemical vapour deposition. Combining gas molecules allows the deposition to occur in a reaction chamber at room temperature. A heated substrate coming into touch with the combined gas causes a chemical reaction. On the substrate surface, this reaction leaves a thin film of product that is collected and can be put to use. The key factor affecting CVD is the substrate temperature. The ability to obtain high-purity, homogeneous, robust, and hard nanoparticles are one of CVD's benefits. However, CVD has drawbacks too, including the equipment requirements and the generation of very hazardous gaseous by-products.

4.6.1.3. Pyrolysis. Pyrolysis is the technique used the most frequently to create nanoparticles on a large scale. It calls for the use of a flame to burn a precursor. The precursor, which might be liquid or vapour, is introduced into the furnace under high pressure through a small hole, where it burns. The nanoparticles are then air categorized from the combustion or by-product gases. Some furnaces create high temperatures for simple evaporation by using laser and plasma rather than a

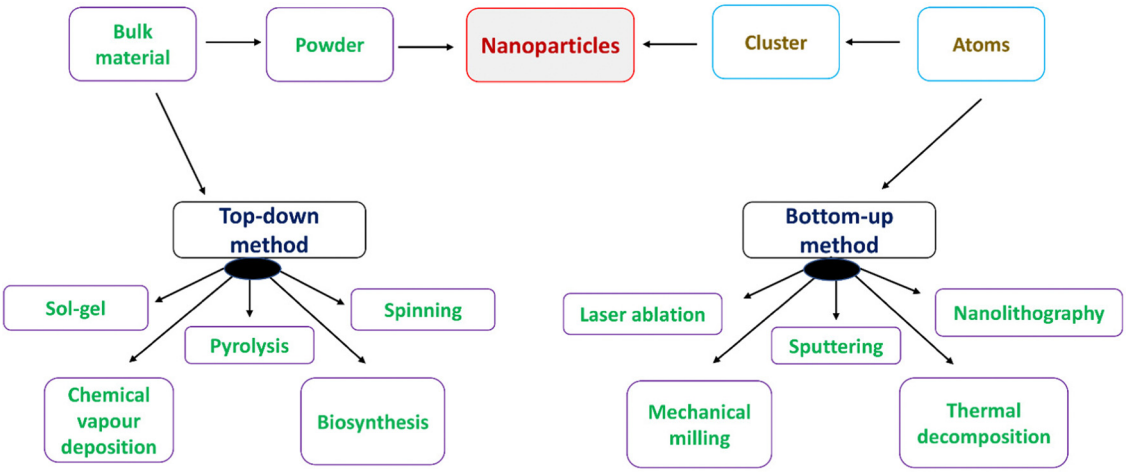

Fig. 9 Common synthesis methods of nanomaterials.

flame. Pyrolysis has the benefits of being a quick, easy, affordable, and continuous process with a high yield.

4.6.1.4. Sol–gel. A colloidal suspension of solids in a liquid phase is known as a sol. A solid macromolecule dissolved in a solvent is the gel. Due to its ease and simplicity with which most nanoparticles can be synthesized, the sol–gel method is the most used bottom-up approach. A chemical solution that serves as a precursor for an integrated system of discrete particles is used in this wet-chemical process. The typical precursors for the sol–gel process are metal oxides and chlorides. The precursor is subsequently mixed with the host liquid by sonication, shaking, or stirring, resulting in a system with a liquid and solid phase. Several methods, including sedimentation, filtering, and centrifugation, are used to recover the nanoparticles after a phase separation, and drying is then used to further remove the moisture.

4.6.1.5. Spinning. A spinning disc reactor produces nanoparticles using spinning synthesis (SDR). It has a spinning disc within a reactor or chamber where the physical characteristics, including temperature, can be regulated. The reactor is often filled with nitrogen or other inert gases to remove oxygen and prevent chemical reactions. Water and the precursor are injected into the disc while it is rotating at a variable speed. As a result of the molecules or atoms joining together due to the spinning, they are precipitated, gathered, and dried. The features of the nanoparticles synthesized from SDR depend on the many operating parameters, including the liquid flow rate, disc rotation speed, liquid/precursor ratio, location of the feed, and disc surface.

4.6.2. Top-down methods

4.6.2.1 Laser ablation. The process of producing nanoparticles from a multitude of solvents is called laser ablation synthesis in solution (LASIS). In this approach, a laser beam's condensing energy causes a plasma plume to form when it strikes a metal submerged in a liquid solution, which results in the production of nanoparticles. It is an effective top-down approach that offers an alternative to the traditional chemical reduction of metals to synthesize metal-based nanoparticles. It is also a "green" process since LASIS offers a stable synthesis route for nanoparticles in water and organic solvents without the need for chemicals or stabilizing agents.

4.6.2.2 Mechanical milling. The most popular top-down technique for creating different nanoparticles is mechanical milling. While creating nanoparticles by this synthesis approach, different components are milled in an inert atmosphere. This method is known as mechanical milling. Plastic deformation, which determines the particle shape; fracture, which reduces the particle size; and cold-welding, which increases the particle size, are the influencing factors in the mechanical milling.

4.6.2.3 Nanolithography. Nanolithography involves creating structures at the nanometre scale with at least one dimension between 1 and 100 nm. There are numerous methods used for nanolithography, including optical, electron-beam, multiphoton, nanoimprint, and scanning probe lithography. Broadly speaking, lithography is the act of imprinting a necessary shape or structure onto a light-sensitive material while only removing a little amount of material to produce the shape and structure needed. The ability to manufacture anything from a single nanoparticle to a cluster with the desired shape and size is one of nanolithography's key advantages. However, its complex equipment requirements and accompanying costs are the drawbacks.

4.6.2.4 Sputtering. Sputtering is the process of ejecting nanoparticles from one surface and depositing them on another surface through particle-ion collisions. Sputtering typically involves depositing a thin coating of nanoparticles and then annealing those particles. The size and shape of the nanoparticles are dependent on the substrate type, temperature, and length of annealing, among other factors.

4.6.2.5 Thermal decomposition. When heat is used to disrupt chemical bonds in a substance, thermal decomposition, an endothermic chemical decomposition, results. The

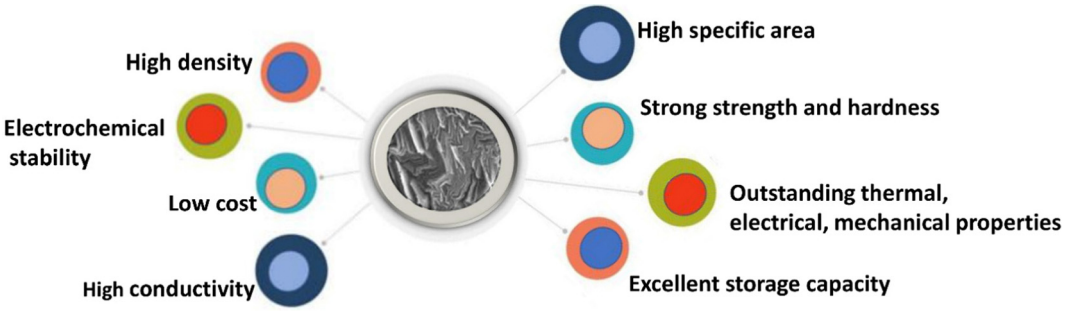

Fig. 10 Schematic showing the different advantages of supercapacitors with carbon materials.

decomposition temperature is the precise temperature at which an element begins to chemically break down, at which point the metal is broken down into tiny particles by undergoing chemical reactions at a certain temperature, which results in by-products like nanoparticles.

4.7. Utilisation of carbon-based materials. Many energy-storage technologies, including fuel cells, batteries,[71] capacitors,[72] and solar cells,[73] have been produced so far. Among these, a British scientist named William Grove invented the fuel cell in 1839, which was the first energy-storage technology capable of producing a significant quantity of energy. Grove's method was used by the National Aeronautics and Space Administration (NASA) to create the first fuel cell that was employed for commercial purposes in 1960. After that, several changes were made to enhance its capacity to produce electricity. Thereafter, researchers have concentrated on electrical energy storage and created many energy-storage technologies, like batteries and capacitors (supercapacitor). The first electronic double-layer capacitors (supercapacitors) were developed and patented by American Oil Corporation and Standard Oil of Ohio in the US in 1961 (SOHIO). Following that, these devices caught researchers' attention greatly, and notable improvements were made in their development, ushering in a new era in energy-storage applications. Researchers have investigated a variety of materials, including carbon-based materials, metal oxides, composites, and hybrids, in order to further improve the storage capacity and stability of these devices. Carbon-based materials have many uses because of their remarkable properties,[74] as shown in the schematic representation in Fig. 10. However, there is currently a sizeable demand for the investigation and creation of novel environmental impact-reduction technologies, with a constant emphasis on the use of affordable, renewable raw materials.

5. Mxene–carbon hybrid materials developed for supercapacitors

Research into supercapacitors has generated a lot of interest in MXenes. However, the convenience and use of surfaces for the storage of electrochemical energy are severely constrained by MXene's inherent inclination to face-to-face restack and random aggregation, which is shared by all other 2D materials. To date, several approaches have been used to deal with the restacking difficulty, most notably the use of additional nanomaterials as spacers in MXene films, usually carbon-based materials, like activated carbon (AC), CNTs, conducting polymers (CPs), and graphene (GO, rGO).

5.1. MXene–carbon nanotube-based hybrid materials for supercapacitors

CNTs are 1D nanostructure materials that were first reported by Iijima in the 1990s, and have since been extensively researched and used as the best candidate for energy storage. They show outstanding thermal, electrical, and mechanical properties, with a large surface-to-weight ratio, large surface area, and excellent capacity storage. The literature review revealed many works that have discussed the use of materials based on CNTs for energy storage.

For instance, L. Yang *et al.*[75] successfully synthesized Ti_3C_2/CNTs nanofilms and effectively deposited them onto graphite paper *via* an electrophoretic deposition (EPD) method, as shown in Fig. 11, and then studied the electrochemical behaviour. According to the authors, the composite demonstrated outstanding cycling stability after 10 000 cycles even at a current density of 5 A g^{-1}, while at a power density of 416.7 W kg^{-1}, the energy density reached 0.56 W h kg^{-1} (Fig. 12). The addition of CNTs to MXene creates a strong framework that keeps MXene from restacking and contributes to its enhanced electrochemical performance. Chen[76] and co-workers fabricated a $Ti_3C_2T_x$ MXene/CNTs composite for application in supercapacitors. They demonstrated that the synthesized material showed a high capacitance of 300 F g^{-1} under a current density of 1 A g^{-1} along with a superior rate performance of 199 F g^{-1} even at 500 A g^{-1}. Moreover, 92% retention of capacitance was reported even after 10 000 cycles under a high current density (20 A g^{-1}), indicating the long cycle stability. The prevention of self-restacking, fast ion diffusion, and outstanding high-rate performance were made possible by incorporating the CNTs into MXene. Ting Zheng *et al.*[77] prepared MXene/CNTs/HA hybrid fibers by a wet-spinning method with sodium hyaluronate (HA) as the dispersant and examined their electrochemical properties. They found that the composite had a volumetric capacitance of 13.95 ± 2.45 F cm^{-3}, and even after 1000 charge–discharge cycles the capacitance retention rate was 82%. MXene/CNT Yarn was made by Zhiyu Wang *et al.*[78] using a

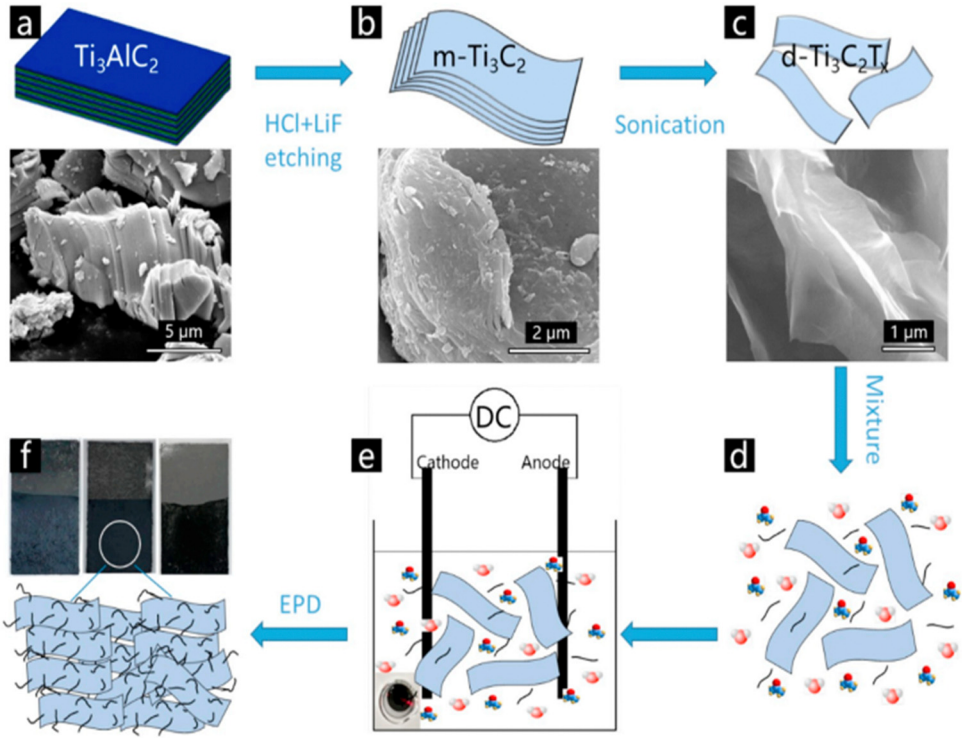

Fig. 11 Illustration of the EPD preparation process for electrode films: (a) morphology of Ti_3AlC_2; (b) morphology of m-Ti_3C_2; (c) morphology of d-Ti_3C_2; (d) solution mixture of DI H_2O and acetone with d-Ti_3C_2 and CNTs; (e) EPD process; (f) sketch and photographs of d-Ti_3C_2 film, Ti_3C_2/CNTs film, and CNTs. Reprinted with permission from ref. 75. Copyright 2018, Elsevier.

biscrolling approach, and its electrochemical characteristics were examined. It was found that the composite exhibited charging and discharging properties over an energy density of 61.6 mW h cm^{-3} and a power density of 5428 mW cm^{-3}, and that the capacitance retention after 10 000 cycles at 20 mA cm^{-2} was close to 100%. This showed it was possible to use a small amount of supercapacitor woven into a textile to power small electrical gadgets. Additionally, the energy-storing textile prototype showed potential for electric integration with flexible and textile-based due to its remarkable performance across several charge–discharge cycles and strong mechanical endurance. Park, Jong Woo and co-workers[79] used the liquid-state biscrolling approach to create an effective electrode material utilizing MXene/CNT and examined its electrochemical performance. They measured a power density of 26 mW cm^{-2} and an energy density of 100 μW h cm^{-2}, as well as a high areal capacitance of 1.56 F cm^{-2}. The biscrolling permitted increasing the MXene weight fraction in the yarn while maintaining its mechanical strength and electrical conductivity. Also, the yarn supercapacitor could continue to function despite mechanical deformation with no performance loss. Pengtao Yan and co-workers[80] synthesized delaminated Ti_3C_2 sheets from MXenes using intercalation and ultrasonication, and utilized CNTs to prevent the sheets from aggregating, and studied the electrochemical performance of the ideal d-Ti_3C_2/CNT. The authors noticed that these electrodes showed excellent performance with a high volumetric capacitance of 393 F cm^{-3} at 5 mV s^{-1}. As the scan rate increased from 5 to 100 mV s^{-1}, the capacitance retention reached 80%, And it showed excellent cyclic stability over metal oxides. By preventing the stacking of Ti_3C_2, extending the space among sheets, and enhancing the electrical conductivity, the addition of CNTs could greatly improve the supercapacitive performance of delaminated Ti_3C_2. As a result, the composite materials made of d-Ti_3C_2 and CNTs had excellent electrochemical characteristics and are extremely promising as pseudocapacitor materials. Qishan Fu[81] reported the synthesis of a $Ti_3C_2T_x$/SCNT self-assembled composite electrode *via* vacuum filtration, which displayed excellent electrochemical properties, with a high areal capacitance of 220 mF cm^{-2} (314 F cm^{-3}) along with 95% capacitance retention after 10 000 cycles. They demonstrated how this material could be used as a high-performing, low-cost energy collector for supercapacitors.

5.2. MXene–graphene-based materials for supercapacitors

Graphene also plays a very important role to overcome the aforementioned problems of supercapacitors owing to its outstanding mechanical, electronic, and thermal properties. As a result, it has become a highly promising material for the creation of energy-storage devices for researchers and industry alike. Graphene has a stronger intersheet van der Waals force of attraction than CNTs, making it a more durable electrode material. The main characteristics that make both materials potential candidates for energy-storage applications include their large surface area, microporosity, and good electrical conductivity.

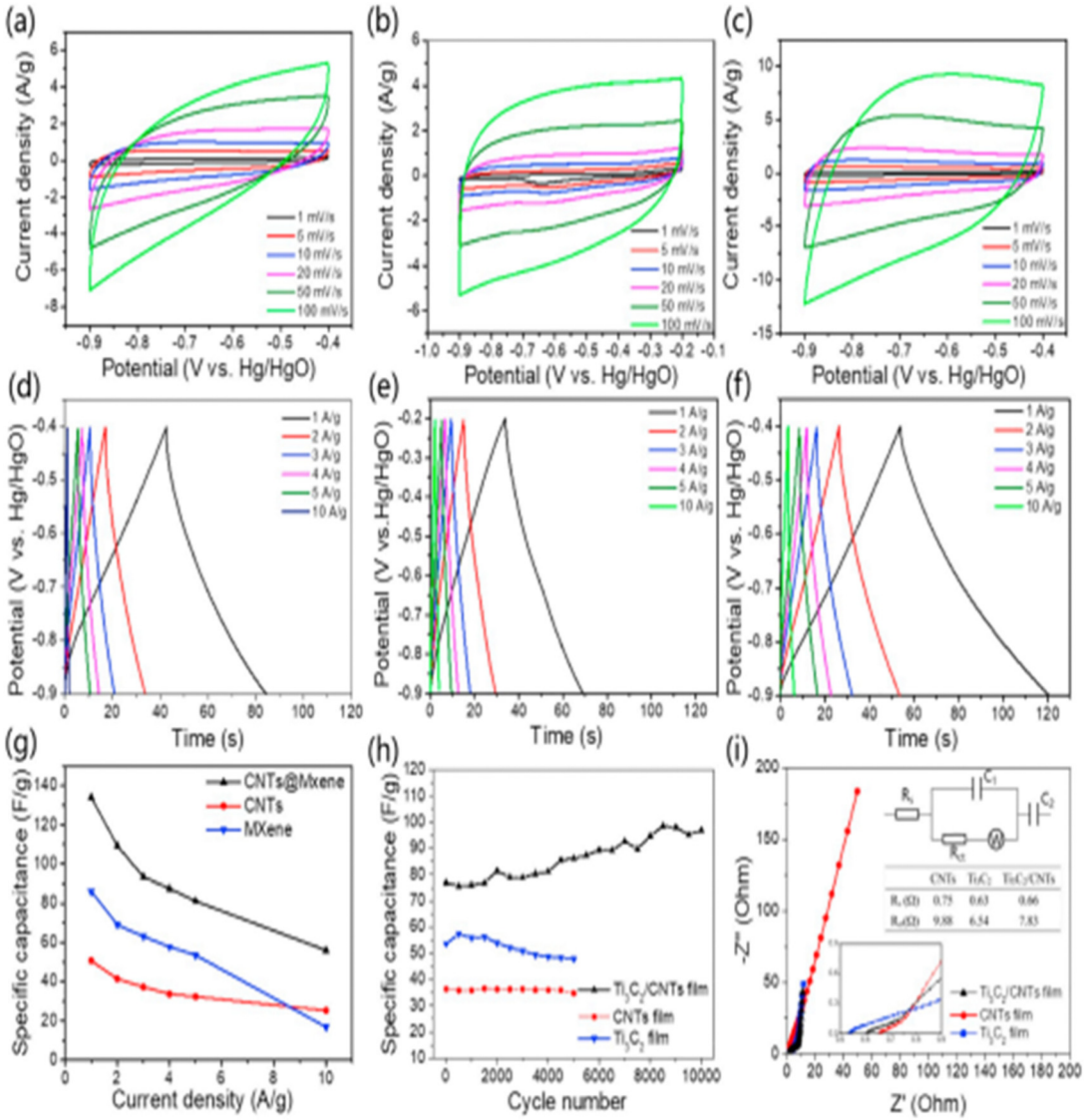

Fig. 12 CV curves of (a) Ti_3C_2 film, (b) CNT film and (c) Ti_3C_2/CNT film at various scan rates; GCD curves of the (d) Ti_3C_2 film, (e) CNT film, and (f) Ti_3C_2/CNT film; (g) plots of the specific capacitance of the three electrodes under different current densities; (h) plots of the specific capacitance of the three electrodes after 10 000 GCD cycles at 5 A g^{-1}; (i) Nyquist plots and the results fitted by the inserted equivalent circuit. Reprinted with permission from ref. 75. Copyright 2018, Elsevier.

In this regard, N. Radha *et al.*[82] carried out a comparative study by synthesizing rGO/Ti_3C_2 composite aerogel film as a freestanding, binder-free, flexible electrode for supercapacitor application. The authors observed that the composite material displayed an outstanding areal capacitance of 41 mF cm^{-2} at a current density of 1 mA cm^{-2}. Whereas a high areal capacitance accompanied by excellent cycle stability with almost no capacitance loss over 1500 cycles at 3 mA cm^{-2} current density was also found. Later on, Pronoy Dutta and co-workers'[83] synthesized a composite film through the graphene-aided gelation of MXene, as shown in Fig. 13 and 14, and investigated its electrochemical properties. The composite film showed a superior excellent gravimetric capacitance of 653.7 F g^{-1} at 2 mV s^{-1}, a very high areal value of 1442 mF cm^{-2}, and volumetric capacitance of ~1522 F cm^{-3}. The hybrid hydrogels exhibited exceptional cyclic stability (<2% decay over 8000 charge–discharge cycles). Due to the composite film's intercalation characteristics, supercapacitors could potentially benefit from it. Min Zhang *et al.*[84] fabricated a reduced graphene oxide/MXene (RGM)–electrolyte composite film that could be used directly as a self-supporting electrode for supercapacitors. The composite films demonstrated a high volumetric capacity of 454.9 F cm^{-3} at 10 mV s^{-1} with a high energy density of 39.4 W h L^{-1}, An outstanding rate capability of 66% capacitance retention at 500 mV s^{-1}, and spectacular cycling stability, as well as good flexibility and electrochemical performance at different bending states and variable working windows. Afterward, Qiuyan Yang, Zhen Xu and group[85] synthesized a hybrid material of MXene and graphene fibers by a wet-spinning technique. The synthesized nanohybrid was then characterized

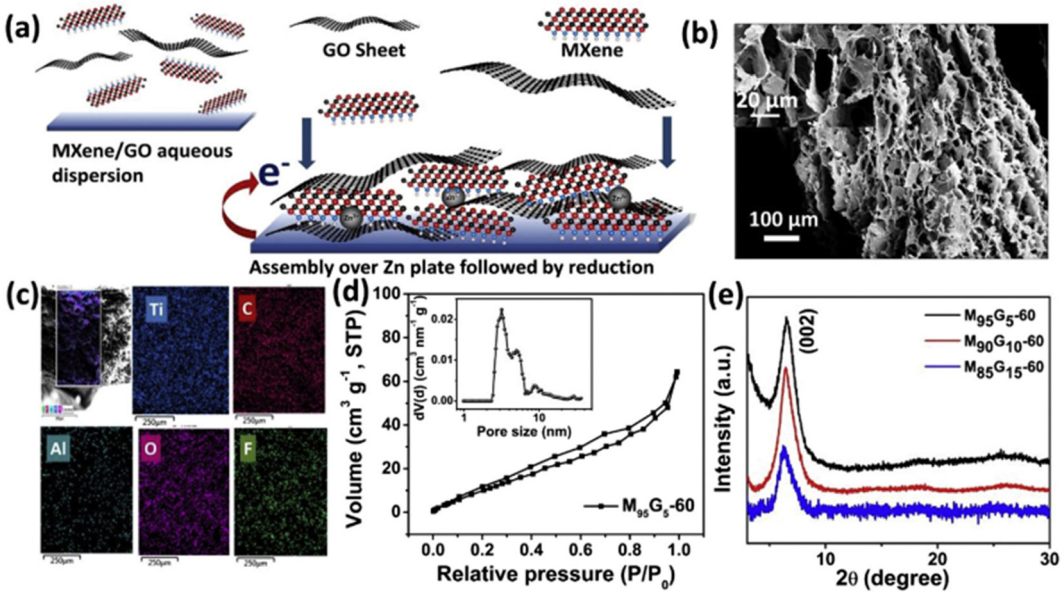

Fig. 13 Development scheme and structural and compositional properties of an MXene–graphene hybrid hydrogel: (a) schematic illustration of layer-by-layer gelation *via* spontaneous assembly and reduction; (b) cross-sectional FESEM image of a freeze-dried hydrogel (M95G5-60) and its higher magnification image in the inset; (c) cross-sectional elemental mapping and (d) N_2 adsorption/desorption isotherms, with pore-size distribution in the inset, for M95G5-60 hydrogel; (e) XRD patterns of hydrogels with different MXene : GO wt% ratios. Reprinted with permission from ref. 83. Copyright 2020, Elsevier.

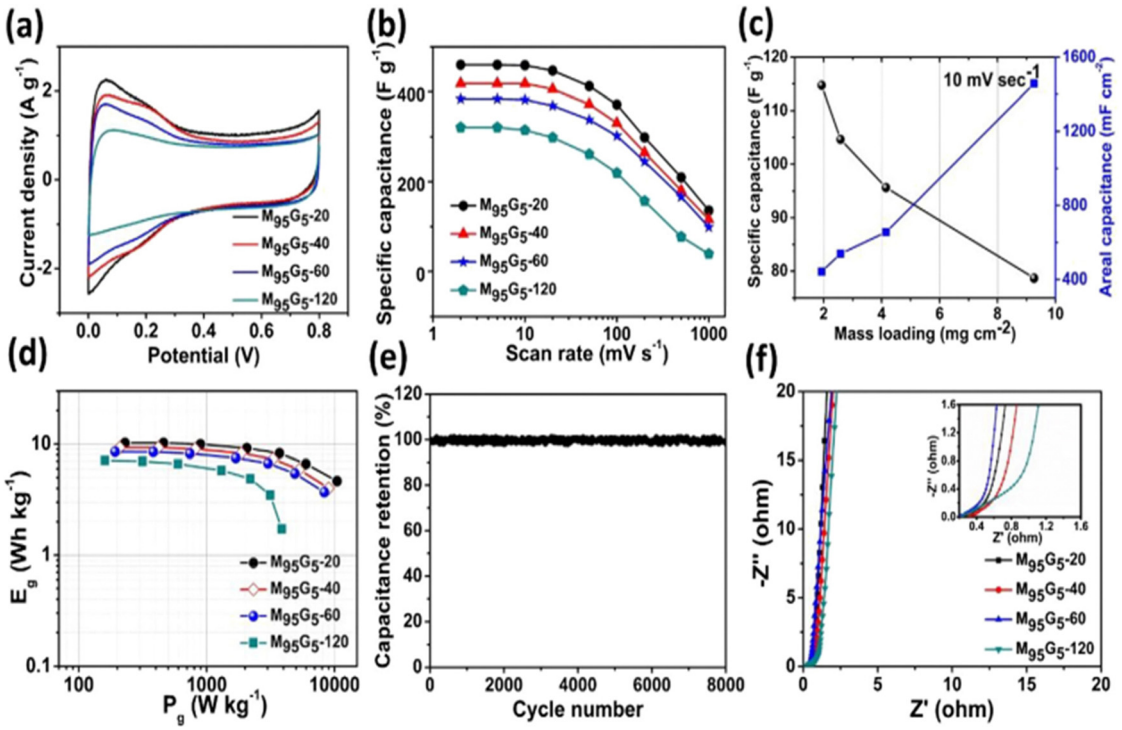

Fig. 14 Energy-storage performance of hybrid hydrogels developed with different gelation times in a symmetric two-electrode device configuration: (a) CV curves at 10 mV s^{1}; (b) gravimetric capacitance of MXene–graphene hybrid electrodes at different scan rates; (c) comparison of the gravimetric and areal capacitance of a device at different mass loadings of electrodes; (d) Ragone plot showing gravimetric energies and power densities; (e) cycling stability of M95G5-20 measured at a constant current charge discharge with a current density of 3 A g^{1} for 8000 cycles; (f) EIS spectra and the inset showing a zoomed-in high-frequency domain. Reprinted with permission from ref. 83. Copyright 2020, Elsevier.

and the authors found that the material had an excellent specific capacitance of 890.7 F cm^{-3} at 10 mV s^{-1}, and highest areal and volumetric capacitance of 372.2 mF cm^{-2} and 586.4 F cm^{-3} at 10 mV s^{-1} with an energy density of 13.03 mW h cm^{-3}

at a power density of 0.59 W cm^{-3}. It also exhibited excellent cycling stability over 3000 cycles, indicating the great potential of such scalable fabricated MXene fibers for applications in portable and wearable electronics. Jun Yan *et al.*[86] prepared a MXene/rGO hybrid electrode film for supercapacitor applications by an electrostatic self-assembly process. The authors noticed that the composite material displayed superb electrochemical properties, with an outstanding volumetric capacitance of 1040 F cm^{-3} at a scan rate of 2 mV s^{-1}. Additionally, the film electrode possessed excellent cycling stability with almost no capacitance decay after 20 000 cycles. Also the fabricated symmetric supercapacitor displayed an ultrahigh volumetric energy density of 32.6 W h L^{-1} and a maximum volumetric power density of up to 74.4 kW L^{-1}, hence an increase in conductivity was observed, which suggests their application potential in supercapacitors.

5.3. MXene–activated carbon-based hybrid materials for supercapacitors

Activated carbon (AC), an additional superior carbon-based material, possesses exceptional electrical conductivity and an extensive surface area, rendering it suitable for energy-storage devices. To optimize the electrochemical properties and ensure only a moderate cost, it is crucial for the AC to possess a high surface area and a narrow pore-size distribution. The incorporation of additional components, such as metal oxides, conducting polymer, and other carbon-based materials, can further enhance the performance of AC, leading to improved energy-storage capabilities.

Lanyoung Yu and collaborators[87] successfully developed an efficient energy-storage material utilizing MXene as a flexible and conductor binder for supercapacitor carbon electrode fabrication, as depicted in Fig. 15. The authors investigated the excellent electrochemical properties of this material, revealing its remarkable performance, including a high capacitance of 126 F g^{-1} and outstanding rate performance, with 57.9% capacitance retention at 100 A g^{-1} in an organic electrolyte, as shown in Fig. 16. Thus, the results surpassed those of both pure MXene and polymer-bonded carbon films, whereby incorporating AC into MXene expanded the distance between the MXene layers, facilitating easier ion and electrolyte infiltration, thereby enhancing the overall performance of the material.

Yapeng Tian *et al.*[88] successfully synthesized materials showing remarkable advancements in the field of high-performance composite with freestanding and flexible $Ti_3C_2T_x$ paper as the anode electrode, alongside flexible AC as the electrode. The materials demonstrated exceptional improvements in terms of stability, cyclability, and overall performance with an outstanding volumetric capacitance of 250 F cm^{-3} at 2 mV s^{-1}, accompanied by a high volumetric energy density of up to 102.8 W h L^{-1} at 424 W L^{-1}, and a first-rate cycling stability with 122% capacitance retention even after 6000 cycles. Further, Li Wang and colleagues[89] reported the synthesis of an HHK-CC (HHK-CC = activated carbon cloth) and MXene electrode using a simple method and investigated the electrochemical performance. The researchers found that these materials exhibited a high capacitance of 1033 mF cm^{-2} at a current density of 1 mA cm^{-2}, and after 1000 cycles, the capacitance was retained at an impressive 94.2%. Additionally, they obtained a high power density of 0.779 W cm^{-2} at a high energy density of 4.5 μW h cm^{-2}. Even when assembled into a symmetrical solid-state supercapacitor, the carbon cloth retained its flexibility and mechanical strength, displaying no significant decrease in capacitance under bending and deformation conditions.

Yue Li *et al.*[90] explored the fabrication of MXene layers and chain-like PANI by a simple hydrothermal reaction. The resulting materials exhibited excellent performance, boasting a high cycle lifespan with a capacitance retention of 95.15% after 10 000 cycles, coupled with a high specific capacity of 563 F g^{-1} at 0.5 A g^{-1} and an excellent capacitance retention rate of 84.72%. Further enhancing the energy density, they

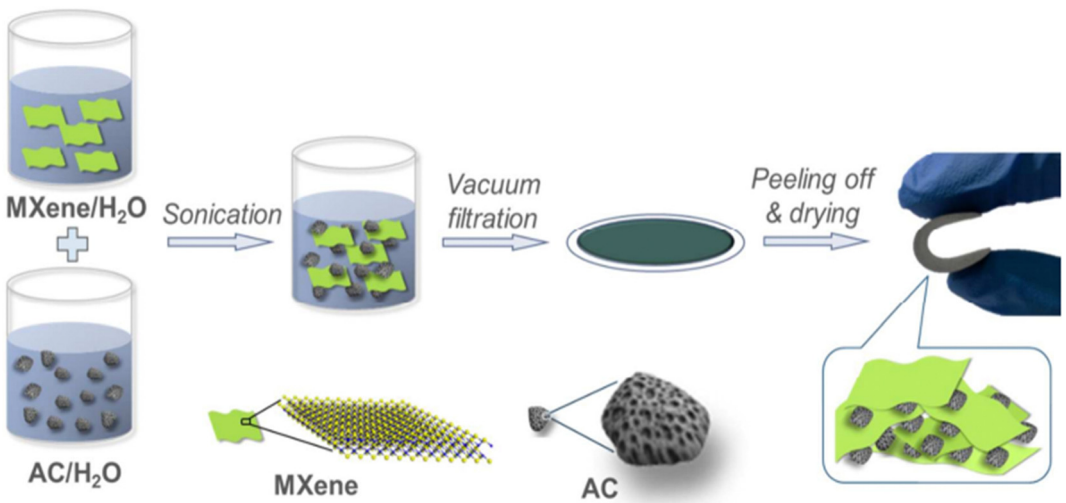

Fig. 15 Schematic showing the process for creating MXene-bonded AC films, which involved dispersing AC particles and MXene flakes in water, followed by a vacuum-assisted filteration, peeling-off of the excess material, and drying. Reprinted with permission from ref. 87. Copyright 2018, American Chemical Society.

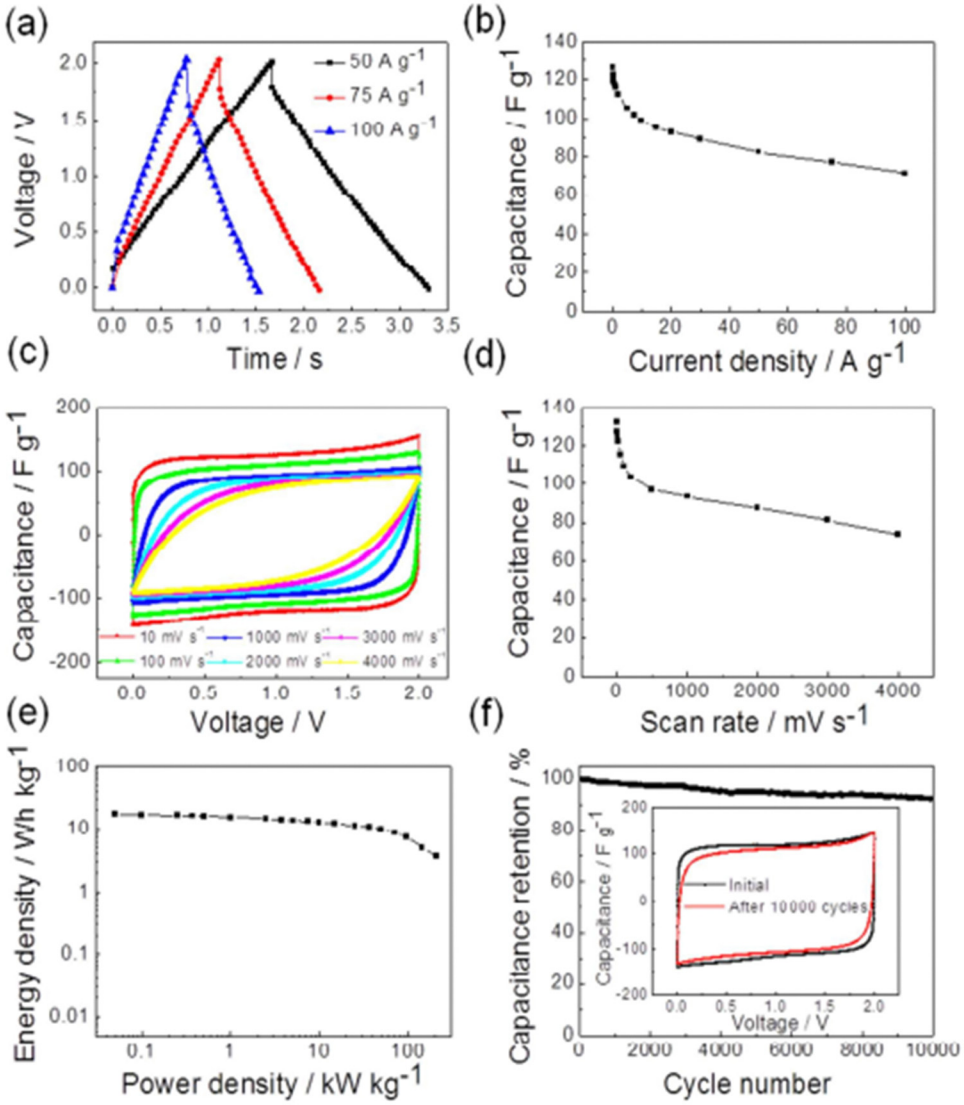

Fig. 16 Electrochemical performance testing results for an AC/MXene-2:1 film. (a) *V*–*T* curves at higher current densities. With a very tiny voltage drop, the AC/MXene-2:1 film could survive rapid charge–discharge at a current density of 100 A g^{-1}. (b) Rate capabilities: the AC/MXene-2 : 1 film presented first-rate performance with a capacitance of 71 F g^{-1} at 100 A g^{-1}. (c) CV curves: the CV curves of the AC/MXene-2 : 1 film could maintain rectangle-like characteristics even at an ultrahigh scan rate of 4000 mV s^{-1}. (d) Capacitance at different scan rates: the AC/MXene-2 : 1 film presented a high capacitance of 73.8 F g^{-1} at 4000 mV s^{-1}. (e) Ragone plots: the AC/MXene-2 : 1 film could output an ultrahigh power density of 207 kW kg^{-1} with a maximum energy density of 17.5 W h kg^{-1}. (f) Cyclic performance at 10 A g^{-1}. The inset in (f) shows the CV curves at a scan rate of 20 mV s^{-1} at the initial cycle and after 10 000 cycles at 10 A g^{-1}. The capacitance retention of the AC/MXene-2 : 1 film was as high as 92.4% after 100 000 cycles at a current density of 10 A g^{-1}, indicating good cyclic stability. All the data are based on the total mass of the AC/MXene-2 : 1 film.

developed an asymmetric supercapacitance based on MXene/PANI hybrids as a positive electrode and active carbon as the negative electrode, accomplishing an energy density of 22.67 W h kg^{-1} at a power density of 0.217 kW kg^{-1}. These aforementioned studies contribute significantly to the field of supercapacitors and demonstrate great promise for upcoming energy-storage applications.

5.4. MXene–conducting polymer-based hybrid materials for supercapacitors

Conducting polymers have also attracted significant attention in the area of supercapacitors owing to their good intrinsic conductivity. Among the most extensively studied conducting polymers are polyaniline (PANI), polypyrrole (PPy), polythiophene (PTh), and poly(3,4-ethylenedioxythiophene) (PEDOT). Conductive polymers are typically conductive under many doping conditions, as they possess a narrower band gap (1–3 eV) than typical polymers (10 eV). Moreover, these polymers have different morphologies, particular doping/undoping behaviours, and relatively quick charge and discharge capabilities.

Ke Li, Xuehang Wang *et al.*[91] fabricated a highly efficient PANI@MXene positive electrode as illustrated in Fig. 17 and 18, and the authors found that it had exceptional volumetric capacitance, reaching 1632 F cm^{-3} at a scan rate of

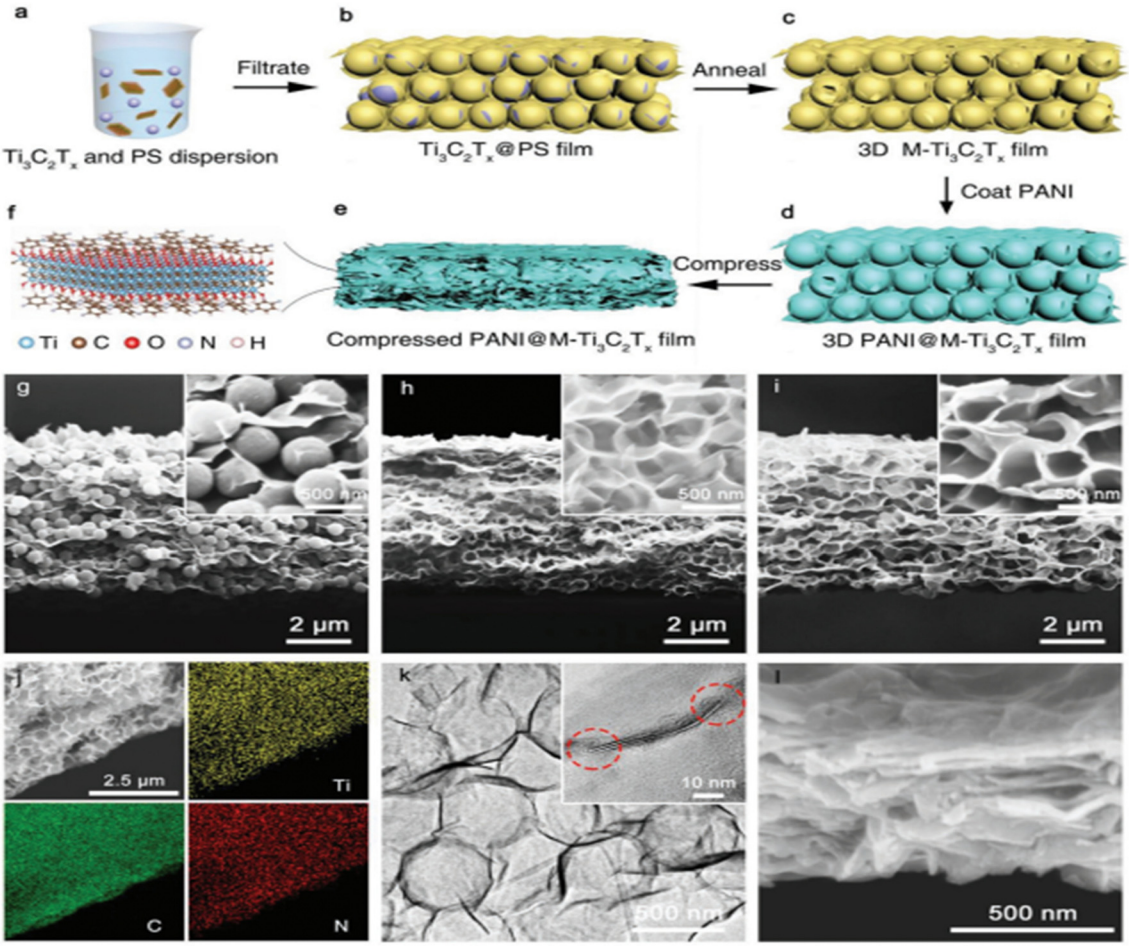

Fig. 17 Schematic showing the preparation of a compressed PANI@M-$Ti_3C_2T_x$ electrode and its corresponding morphology: (a) $Ti_3C_2T_x$ flakes and PS spheres are added to form a uniform colloidal solution, (b) a freestanding $Ti_3C_2T_x$@PS film is obtained through filtration, (c) a 3D M-$Ti_3C_2T_x$ film is obtained using the annealing process for eliminating the PS spheres, (d) PANI solution is dropped onto 3D PANI@M-$Ti_3C_2T_x$, dried, and then shaped into a 3D PANI@M-$Ti_3C_2T_x$, (e) a compressed film of PANI@M-$Ti_3C_2T_x$ film is obtained, and finally (f) PANI is deposited on the two surfaces of $Ti_3C_2T_x$. SEM cross-sectional pictures of (g) $Ti_3C_2T_x$@PS, (h) 3D M-$Ti_3C_2T_x$, and (i) 3D PANI@M-$Ti_3C_2T_x$. (j) Energy dispersive X-ray spectrometry mapping of 3D PANI@M-$Ti_3C_2T_x$ film. (k) TEM images of 3D PANI@M-$Ti_3C_2T_x$. (l) Compressed PANI@M-$Ti_3C_2T_x$ film Cross-sectional SEM image. Reprinted with permission from ref. 91. Copyright 2019, John Wiley and Sons.

10 mV s^{-1}, with remarkable capacitance retention, maintaining 827 F cm^{-3} even at high scan rate up to 5000 mV s^{-1}. Additionally, they synthesized an asymmetric device utilizing PANI@MXene as the cathodic and MXene as the anodic, resulting in an impressive energy density of 50.6 W h L^{-1} and a power density of 127 kW L^{-1}. Further, Chao Zhang and colleagues[92] developed a hybrid combining MXene and polypyrene, which exhibited great potential in planar supercapacitor applications. They demonstrated that the hybrid material displayed a superior areal capacitance of 109.4 mF cm^{-2} in 2 M H_2SO_4 and 86.7 mF cm^{-2} in PVA/H_2SO_4 at a current density 1.05 mA cm^{-2} with excellent areal energy density of 3.398 μW h cm^{-2} at a power density of 0.0845 mW cm^{-2} and 2.028 μW h cm^{-2} at a high power density of 0.338 mW cm^{-2}. Moreover, the hybrid material exhibited excellent cycling stability with 96% capacitance retention after 10 000 cycles. Afterwards, Li-Ge Gong *et al.*[93] fabricated a hybrid composite comprising covalent polymer chains and ethylenediamine acting as MXene $\{AlW_{12}O_{40}\}$ hybrid composite, and thoroughly investigated the electrochemical performance of the composite material for energy storage. Their findings revealed that the composite material exhibited an outstanding specific capacity (625.99 F g^{-1}), along with high retention ability (95%) even after 5000 cycles. It also displayed a maximum energy density of 6.32 W h kg^{-1} at a power density of 237 W kg^{-1}, highlighting its remarkable energy-storage capabilities. Afterward, Muhammad Boota *et al.*[94] fabricated CP@rGO//MXene; whereby they deposited conducting polymers (CP), including PANI, PPy, and PEDOT, onto rGO sheets *via* oxidative polymerization. The resulting composite materials showed excellent stability with a good cyclic ability, *i.e.* 88% retention after 20 000 cycles. Moreover, the PANI-containing asymmetric devices demonstrated a high power performance, considerable energy density, and the ability to operate within a voltage window up to 1.45 V. Notably these devices achieved a high energy density of approximately 17 W h kg^{-1}, ranking among the highest reported for

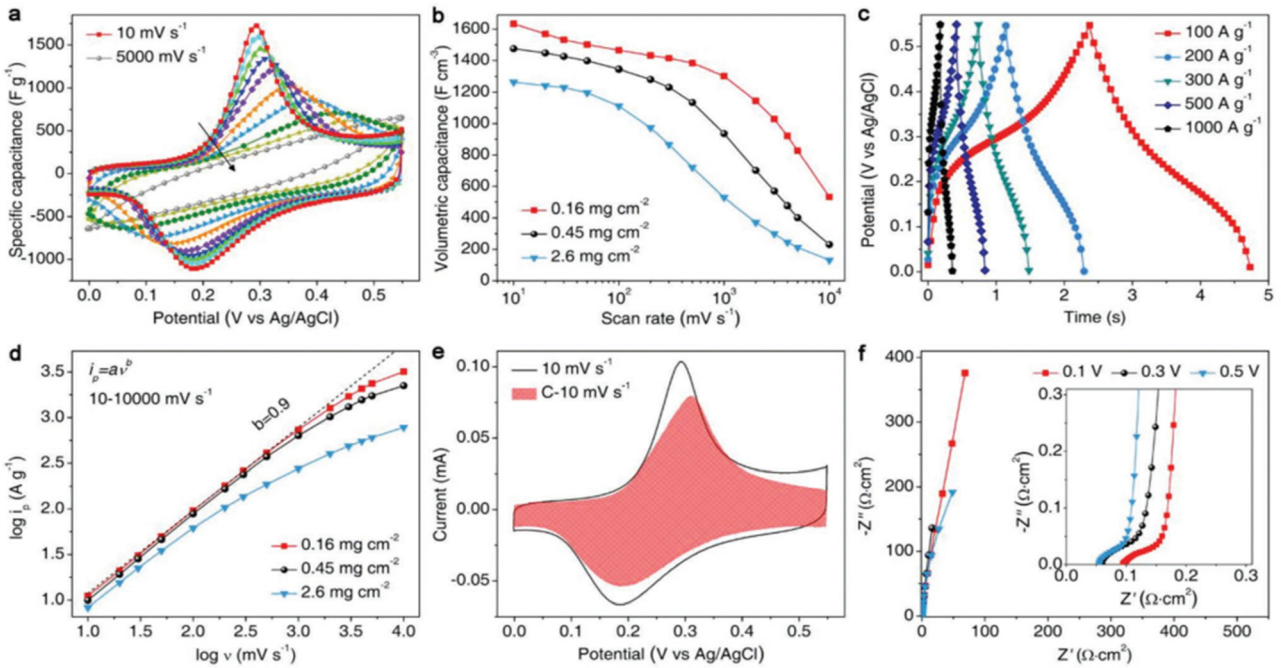

Fig. 18 Compressed PANI@M-$Ti_3C_2T_x$ electrode electrochemical performance. (a) Cyclic voltammetry profiles of the PANI@M-$Ti_3C_2T_x$ film at 10, 20, 50, 100, 200, 500, 1000, 2000, 3000, and 5000 mV s^{-1} with 40 wt% PANI (total mass loading of 0.16 mg cm^{-2}). (b) Volumetric capacitance tests, where the rate performance of PANI@M-$Ti_3C_2T_x$ films at various mass loadings is depicted. (c) PANI@M-$Ti_3C_2T_x$ film (0.16 mg cm^2) galvanostatic charge–discharge curves at high current densities. (d) PANI@M-$Ti_3C_2T_x$ films' *b*-values for various mass loadings calculated using the maximum discharge current value at a scan rate between 10 and 10 000 mV per second. (e) Hatching regions of the CV profiles of the PANI@M-$Ti_3C_2T_x$ film (0.16 mg cm^{-2}) obtained at 10 mV s^{-1} representing the current contributions from the surface capacitive. (f) PANI@M-$Ti_3C_2T_x$ film's (0.16 mg cm^{-2}) electrochemical impedance spectroscopy results obtained at various potentials. Reprinted with permission from ref. 91. Copyright 2019, John Wiley and Sons.

both MXene-based and PANI-containing asymmetric devices. This breakthrough paves the way for integrating various nanostructured CPs with a wide range of readily available MXenes as anode and cathode materials, which can enhance the energy-storage functionality of devices. Subsequently Wenyu Shao and co-workers[95] prepared a PET@MXene NCY hybrid material and investigated its electrochemical properties. The hybrid material exhibited an outstanding specific capacitance of 18.39 mF cm^{-2} at 5 mV s^{-1} while also demonstrating good mechanical properties. Furthermore, the hybrid material displayed superior cycling stability, with a capacitance retention of 98.2% after 6000 cycles and showcased a power density of up to 0.39 mW cm^{-2} at an energy density of 0.38 μW h cm^{-2}, with its outstanding characteristics positioning the hybrid material as a promising candidate for supercapacitor application. By using additional active materials, like graphene, conducting polymers, and others in the nanofibers spinning solutions, these stated values could even be enhanced.

5.5. MXene–carbon fiber hybrid materials for supercapacitors

Carbon fiber materials made from natural biomaterials have attracted a lot of attention because of their enormous scale, low price, superior electrical conductivity, and advantages for the environment. Sun *et al.*[96] have fabricated a hierarchically porous "skin/skeleton"-like MXene/CF for a heterostructure using a single-step pyrolysis of CFW impregnated *via* MXene solution. They studied the electrochemical properties of the electrode and found it exhibited impressive cyclic stability with 99.8% retention after 5000 cycles, a volumetric capacitance of 7.14 F cm^{-3}, and 63.9% retention in capacitance from 0.5 to 100 A g^{-1} together with extended durability and good flexibility. Even after 2500 cycles at various bending angles, the electrode exhibited an impressive cyclic stability, whereby the device still maintained a stable capacitance and structural integrity. In a different study, Liyuan Qin and co-workers[97] developed flexible CNF/MX hybrid aerogels using a liquid nitrogen-assisted unidirectional freezing methodology. The synthesized composite displayed enhanced stability and capacitance, marking it as a top choice for supercapacitor applications. The specific capacitance of the electrode exhibited remarkable performance by maintaining 80% of the capacitance as the current density was raised from 1 to 100 A g^{-1}, and a capacitance retention of 90% could be sustained even after an extensive 20 000 cycles at 5 A g^{-1}. It also displayed an outstanding rate capability and cycling stability, accompanied by an impressive strain capacity of 95% for 500 cycles. Additionally, it exhibited long-term durability with sustained enlargement at 50% strain for at least 5000 cycles. Consequently, Ariana S. Levitt *et al.*[98] used the electrospinning method and fabricated $Ti_3C_2T_x$ MXene/carbon nanofiber electrodes; whereby MXene flakes were combined with carbon nanofiber to create freestanding, highly surface-area abrasive particles, and then examined their electrochemical performance. The synthesized composite materials showed a high areal capacitance of up to 205 mF cm^{-2} at a scan rate of

Table 1 Performance evaluation of diverse MXene–carbon-based hybrid materials for supercapacitors

Sl no.	Material	Specific capacitance	Power density at specified energy density	Capacitance retention	Ref.
1	HHK-CC@$Ti_3C_2T_x$	1033 mF cm^{-2} at current density of 1 mA cm^{-2}	Power density of 0.779 W cm^{-2} at an energy density of 4.5 μW h cm^{-2}	94.2% after 1000 cycles	99
2	Ti_2C/OLC	984.5 F cm^{-3} at current density of 2 mV s^{-1}	Power densities between 0.5 and 5 A g^{-1}	~80% to >95%	100
3	CDs/MXene	984.5 F cm^{-3} at current density of 2 mV s^{-1} landmark rate capacity (79.80%)	Energy density of 19.42 W h kg^{-1}	94.6% after 10 000 cycles	101
4	$Ti_3C_2T_x$/SWCNT	High areal capacitance of 220 mF cm^{-2}	—	95% after 10 000 cycles	102
5	MXene/L-DEA	Capacitance of 503.7 F g^{-1}	Energy density of 51.9 W h kg^{-1} at a power density of 338.5 W kg^{-1}	86% after 10 000 cycle	103
6	rGO:$Ti_3C_2T_x$	254 F g^{-1} at current density of 2 mV s^{-1} and 193 F g^{-1} at current density of 100 mV s^{-1}	—	Long-term cycling stability	104
7	$Ti_3C_2T_x$–RGO	505 F g^{-1} at current density of 2 mV s^{-1}	—	Long-term cycling stability	105
8	MX-CMP	Capacitance value of 72 mF cm^{-2} at 0.25 mA cm^{-2}	Energy density values of 92 and 35 μW h cm^{-2} at power densities of 0.75 and 11 mW cm^{-2}	Long-term stability >5000 cycles	106
9	C@Ti_3C_2	250.6 F g^{-1} at current density of 1 A g^{-1}	Energy density as high as 10.8 W h kg^{-1}	94% after 5000 cycles	107
10	d-Ti_3C_2/rGO	247 F g^{-1} (~445.2 F cm^{-3}) at current density of 1 A g^{-1}	Maximum energy density of 15.7 W h kg^{-1} and a power density 3738.7 W kg^{-1}	Long-term cycling stability	108
11	Se$Ti_3C_2T_x$@N–C	260 F g^{-1} at current density of 0.8 A g^{-1}	—	90% after 5000 cycles	109
12	$Ti_3C_2T_x$/CNF/PC	143 mF cm^{-2} at current density of 0.1 mA cm^{-2}	Energy density of 2.4 μW h cm^{-2} at a power density of 17.5 μW cm^{-2}	~50% after increasing the power density by ~100-fold	110
13	MXene-knotted CNT	Capacitance of 130 F g^{-1}	Energy density of 59 W h kg^{-1} and a power density of 9.6 kW kg^{-1}	Highly stable after 1000 cycles	111
14	CSC@$Ti_3C_2T_x$	Capacitance of 362 mF cm^{-2}	Energy density of 13 μW h cm^{-2} responding to a power density of 181 μW cm^{-2}	96% after 1000 cycles	112
15	$Ti_3C_2T_x$@CCT negative electrode wrapped by $NiCo_2S_4$@CNT positive electrode	559.3 mF cm^{-2} at current density of 5 mV s^{-1}	Energy density of 174.78 μW h cm^{-2}	Long-term cycling stability	113
16	MWCNTs–MXene@CC	114.58 mF cm^{-2} at current density of 5 mV s^{-1}	Energy density of 22.11 mW h cm^{-3} at a power density of 2.99 W cm^{-3}	Long-term stability after 16 000 cycles	114
17	$Ti_3C_2T_x$@CNTs	Capacitance of 201 F g^{-1}	Energy density of 14.0 W h kg^{-1} with a power density of 486 W kg^{-1}	78.1% after 10 000 cycles	115
18	MX/CNS	Capacitance of 180 F g^{-1}	Specific power 37.6 kW kg^{-1} and specific energy 14.1 W h kg^{-1}	Long-term cycling stability	116
19	$Ti_3C_2T_x$/C	364.3 F g^{-1} at current density of 1 A g^{-1}	—	99% after 10 000 cycles	117
20	$Ti_3C_2T_x$ nanosheets/$Ti_3C_2T_x$ quantum dots/RGO	53.1 F cm^{-3} at current density of 50 mA cm^{-3}	Energy density of 16.6 mW h cm^{-3} at a power density of 37.5 mW cm^{-3}	96.6% after 5000 cycles	118
21	NiMX//EMAC	Capacitances of 474.3 and 575.8 F g^{-1},	Energy density of 47.6 W h kg^{-1} at a 375 W kg^{-1} power density	81.7% capacitance retention after 30 000 cycles	119
22	$Ti_3C_2T_x$ MXene/reduced graphene oxide aerogel	Capacitance 1633 F g^{-1} at 1 A g^{-1}	—	86.6% after 10 000 charge	120
23	MXene ($Ti_3C_2T_x$)/CNF/polyaniline (PANI)	Specific capacitance of 2935 mF cm^{-2} at 1 mA cm^{-2}	Energy density of 94.7 μW h cm^{-2} and a high areal power density of 573 μW cm^{-2}	94% after 2000 cycles	121
24	Co_3O_4@NF//MX-5@PCNF	Capacitance of 572.7 F g^{-1} at 1 A g^{-1}	Energy densities of 22.53 W h kg^{-1} and 74.2 W h kg^{-1}	96.4% after 10 000 cycles	122

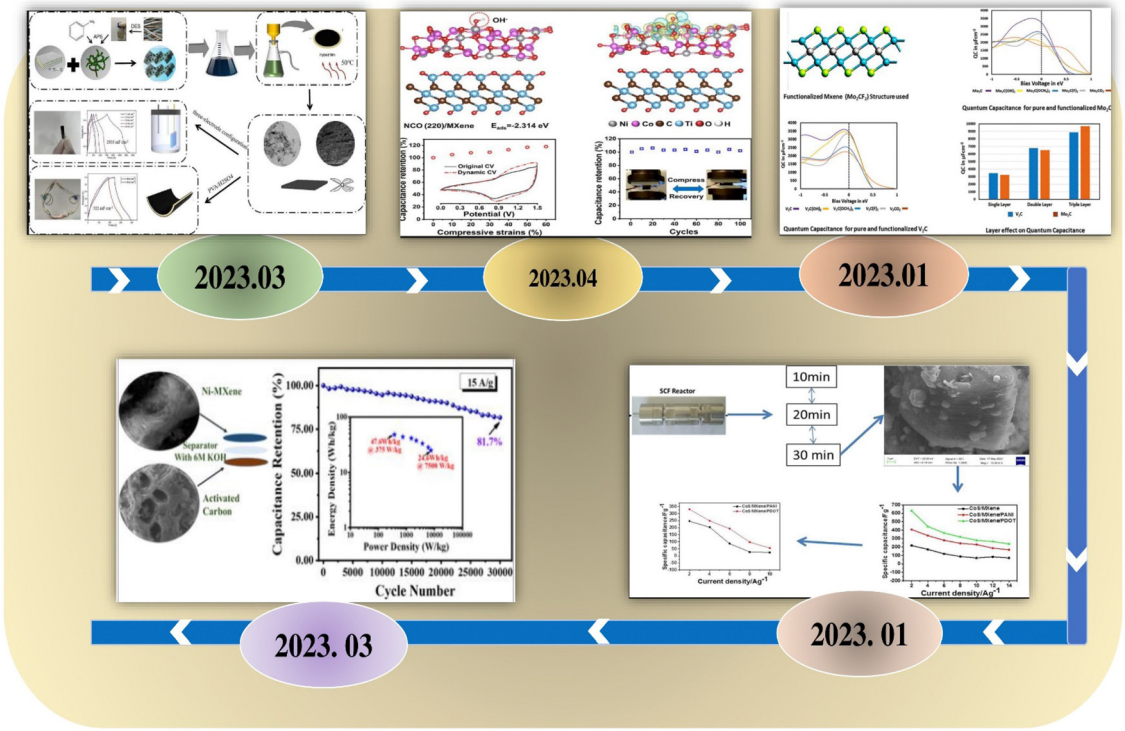

Fig. 19 Development history of MXenes–carbon in flexible supercapacitors. Reproduced from ref. 119 with permission from Elsevier, copyright 2023. Reproduced from ref. 120 with permission from Elsevier, copyright 2023. Reproduced from ref. 121 with permission from Elsevier, copyright 2023. Reproduced from ref. 122 with permission from Elsevier, copyright 2023. Reproduced from ref. 123 with permission from the American Chemical Society, copyright 2023.

50 mV s^{-1}, thus exhibiting versatility for various applications, including filtration, adsorption, and electrocatalysis, where desirable properties such as a high aspect ratio, accessible surface area, and porosity are crucial.

Another important kind of carbon is fullerene, in which the carbon atoms are intricately interconnected through both single and double bonds forming a cohesive mesh-like arrangement. Due of their chemical and heat resistance, fullerenes have attracted significant attention since their discovery in 1985, with their excellent conducting qualities making it possible for them to be used in energy-storage systems. Table 1 provides a thorough analysis of several MXene–carbon-based materials with regard to their performance and application (Fig. 19).

6. Summary and perspectives

Supercapacitors have received significant attention among the different energy-storage solutions due to their unique attributes, including rapid charge–discharge, excellent power density, and excellent cycle life compared to many others. The present review deals with MXene and carbon-based materials for SCs. Even though MXenes come with a number of challenges, this new generation of MXene–carbon based materials is nevertheless advantageous due to their remarkable thermal, electrical, and mechanical properties, making them particularly intriguing for electrochemical energy-storage applications in supercapacitor technology. In this review, the latest progress of MXene–carbon-based materials in SCs were comprehensively summarized. First, the fundamental principles of supercapacitors, such as the types, mechanisms, and advantages, were introduced. Subsequently, MXene–carbon hybrid nanocomposite synthesis methods, competitive features, *etc.* were introduced. Finally, the challenges and perspectives of MXene–carbon-based materials in supercapacitors was proposed. Works to improve the energy-storage performance of MXene hybrid are still in progress. Relevant works show an obvious improvement in performance trend year by year. Although much work has been carried out in this field already, there are still many challenges limiting the commercial applications (Fig. 20). Some major future goals have been taken out from this current audit and shown below instead for reference.

- The current synthesis of MXenes uses HF etchant, which is harmful to human beings and the environment, hence designing safer etchants and environmentally friendly techniques are important for the scalable production of MXenes.
- With the standardization of MXene characterization routes, the improved understanding will benefit the development of flexible MXene materials for realizing satisfactory electrochemical performance towards practical applications.

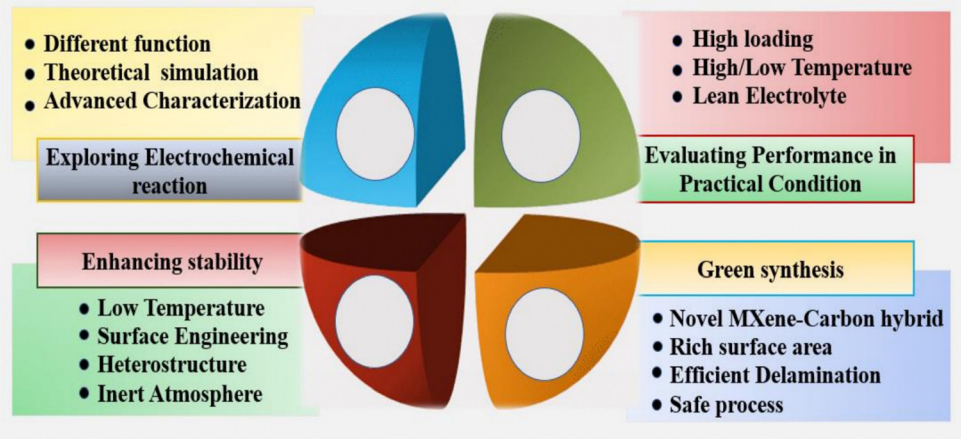

Fig. 20 Future potential directions of MXene–carbon hybrids for supercapacitors.

• Crucial for flexible MXene-based materials operating at extreme conditions, like high/low temperature, lean electrolyte addition, high area mass loading, *etc.* is a detailed understanding of the electronic, optical, magnetic, and quantum confinement effects on the performance of MXene-based devices.

• A holistic evaluation should be adopted in designing flexible MXenes, and transparent and miniaturized MXene-based supercapacitors by understanding the surface chemistry, tunability, and interlayer structures.

Conflicts of interest

Authors declare no conflict of interest.

Acknowledgements

The authors gratefully acknowledge financial assistance from the SERB Core Research Grant (Grant no. CRG/2022/000897), Department of Science and Technology (DST/NM/NT/2019/205(G)), and Minor Research Project Grant, Jain University (JU/MRP/CNMS/29/2023). CSR acknowledges National Research Foundation of Korea for the Brain Pool program funded by the Ministry of Science and ICT, South Korea (Grant no. RS-2023-00222186).

References

1 S. Najib and E. Erdem, Current progress achieved in novel materials for supercapacitor electrodes: mini review, *Nanoscale Adv.*, 2019, **1**(8), 2817–2827.
2 M. Cui and X. Meng, Overview of transition metal-based composite materials for supercapacitor electrodes, *Nanoscale Adv.*, 2020, **2**(12), 5516–5528.
3 Z. S. Iro, C. Subramani and S. S. Dash, A brief review on electrode materials for supercapacitor, *Int. J. Electrochem. Sci.*, 2016, **11**(12), 10628–10643.
4 W. Zuo, R. Li, C. Zhou, Y. Li, J. Xia and J. Liu, Battery-supercapacitor hybrid devices: recent progress and future prospects, *Adv. Sci.*, 2017, **4**(7), 1600539.
5 I. Chotia and S. Chowdhury, Battery storage and hybrid battery supercapacitor storage systems: A comparative critical review, 2015 IEEE Innovative Smart Grid Technologies-Asia (ISGT ASIA), 2015, pp. 1–6.
6 M. Lu, *Supercapacitors: materials, systems, and applications*, John Wiley & Sons, 2013.
7 J. Libich, J. Máca, J. Vondrák, O. Čech and M. Sedlaříková, Supercapacitors: Properties and applications, *J. Energy Storage*, 2018, **17**, 224–227.
8 P. Sinha and K. K. Kar, Introduction to supercapacitors, in *Handbook of Nanocomposite Supercapacitor Materials II: Performance*, Springer International Publishing, Cham, 2020, pp. 1–28.
9 J.-C. Lei, X. Zhang and Z. Zhou, Recent advances in MXene: Preparation, properties, and applications, *Front. Phys.*, 2015, **10**, 276–286.
10 X. Zhan, C. Si, J. Zhou and Z. Sun, MXene and MXene-based composites: synthesis, properties and environment-related applications, *Nanoscale Horiz.*, 2020, **5**(2), 235–258.
11 Q. Zhong, Y. Li and G. Zhang, Two-dimensional MXene-based and MXene-derived photocatalysts: Recent developments and perspectives, *Chem. Eng. J.*, 2021, **409**, 128099.
12 S. Iqbal, H. Khatoon, A. H. Pandit and S. Ahmad, Recent development of carbon-based materials for energy storage devices, *Mater. Sci. Energy Technol.*, 2019, **2**(3), 417–428.
13 M. Lu, *Supercapacitors: materials, systems, and applications*, John Wiley & Sons, 2013.
14 D.-G. Wang, Z. Liang, S. Gao, C. Qu and R. Zou, Metal-organic framework-based materials for hybrid supercapacitor application, *Coord. Chem. Rev.*, 2020, **404**, 213093.
15 S. Saini, P. Chand and A. Joshi, Biomass derived carbon for supercapacitor applications, *J. Energy Storage*, 2021, **39**, 102646.
16 Z.-Y. Li, P. T. M. Bui, D.-H. Kwak, M. S. Akhtar and O.-B. Yang, Enhanced electrochemical activity of low temperature solution process synthesized Co_3O_4 nanoparticles for

pseudo-supercapacitors applications, *Ceram. Int.*, 2016, **42**(1), 1879–1885.
17 S. Najib and E. Erdem, Current progress achieved in novel materials for supercapacitor electrodes: mini review, *Nanoscale Adv.*, 2019, **1**(8), 2817–2827.
18 S. B. Aziz, F. Ali, H. Anuar, T. Ahamad, W. O. Kareem, M. A. Brza and M. F. Z. Kadir, *et al.*, Structural and electrochemical studies of proton conducting biopolymer blend electrolytes based on MC: Dextran for EDLC device application with high energy density, *Alexandria Eng. J.*, 2022, **61**(5), 3985–3997.
19 P. Sharma and T. S. Bhatti, A review on electrochemical double-layer capacitors, *Energy Convers. Manage.*, 2010, **51**(12), 2901–2912.
20 Y.-J. Kim, Y. Masutzawa, S. Ozaki, M. Endo and M. S. Dresselhaus, PVDC-based carbon material by chemical activation and its application to nonaqueous EDLC, *J. Electrochem. Soc.*, 2004, **151**(6), E199.
21 L. Guo, M. Ding, D. Yan, M. E. Pam, S. Vafakhah, C. Gu, W. Zhang, P. V. Y. Alvarado, Y. Shi and H. Y. Yang, High speed capacitive deionization system with flow-through electrodes, *Desalination*, 2020, **496**, 114750.
22 E. Faggioli, P. Rena, V. Danel, X. Andrieu, R. Mallant and H. Kahlen, Supercapacitors for the energy management of electric vehicles, *J. Power Sources*, 1999, **84**(2), 261–269.
23 Ali Eftekhari, The mechanism of ultrafast supercapacitors, *J. Mater. Chem. A*, 2018, **6**(7), 2866–2876.
24 K.-W. Nam and K.-B. Kim, A study of the preparation of NiO_x electrode via electrochemical route for supercapacitor applications and their charge storage mechanism, *J. Electrochem. Soc.*, 2002, **149**(3), A346.
25 N. R. Chodankar, H. D. Pham, A. K. Nanjundan, J. F. S. Fernando, K. Jayaramulu, D. Golberg, Y.-K. Han and D. P. Dubal, True meaning of pseudocapacitors and their performance metrics: asymmetric versus hybrid supercapacitors, *Small*, 2020, **16**(37), 2002806.
26 D. P. Dubal, O. Ayyad, V. Ruiz and P. Gomez-Romero., Hybrid energy storage: the merging of battery and supercapacitor chemistries, *Chem. Soc. Rev.*, 2015, **44**(7), 1777–1790.
27 D. P. Chatterjee and A. K. Nandi, A review on the recent advances in hybrid supercapacitors, *J. Mater. Chem. A*, 2021, **9**(29), 15880–15918.
28 A. Muzaffar, M. Basheer Ahamed, K. Deshmukh and J. Thirumalai., A review on recent advances in hybrid supercapacitors: Design, fabrication and applications, *Renewable Sustainable Energy Rev.*, 2019, **101**, 123–145.
29 C. Zhan, X. Zeng, X. Ren, Y. Shen, R. Lv, F. Kang and Z.-H. Huang, Dual-ion hybrid supercapacitor: Integration of Li-ion hybrid supercapacitor and dual-ion battery realized by porous graphitic carbon, *J. Energy Chem.*, 2020, **42**, 180–184.
30 Y. Ma, H. Chang, M. Zhang and Y. Chen, Graphene-based materials for lithium-ion hybrid supercapacitors, *Adv. Mater.*, 2015, **27**(36), 5296–5308.
31 J. Zhang and X. S. Zhao, On the configuration of supercapacitors for maximizing electrochemical performance, *ChemSusChem*, 2012, **5**(5), 818–841.
32 K. Nasrin, V. Sudharshan, K. Subramani and M. Sathish, Insights into 2D/2D MXene heterostructures for improved synergy in structure toward next-generation supercapacitors: A review, *Adv. Funct. Mater.*, 2022, **32**(18), 2110267.
33 Y. Wu, W. Yuan, M. Xu, S. Bai, Y. Chen, Z. Tang and C. Wang, *et al.*, Two-dimensional black phosphorus: Properties, fabrication and application for flexible supercapacitors, *Chem. Eng. J.*, 2021, **412**, 128744.
34 S. K. A. Raj, P. Mane, S. Radhakrishnan, B. Chakraborty and C. S. Rout, Heterostructured Metallic 1T-VSe_2/$Ti_3C_2T_x$ MXene Nanosheets for Energy Storage, *ACS Appl. Nano Mater.*, 2022, **5**(3), 4423–4436.
35 J. Zheng, X. Pan, X. Huang, D. Xiong, Y. Shang, X. Li, N. Wang, W.-M. Lau and H. Y. Yang, Integrated NiCo2-LDHs@MXene/rGO aerogel: componential and structural engineering towards enhanced performance stability of hybrid supercapacitor, *Chem. Eng. J.*, 2020, **396**, 125197.
36 X. Liu, F. Xu, Z. Li, Z. Liu, W. Yang, Y. Zhang, H. Fan and H. Ying Yang, Design strategy for MXene and metal chalcogenides/oxides hybrids for supercapacitors, secondary batteries and electro/photocatalysis, *Coord. Chem. Rev.*, 2022, **464**, 214544.
37 S. Zhang, Y. Huang, J. Wang, X. Han, C. Chen and X. Sun., $Ti_3C_2T_x$/g-C_3N_4 heterostructure films with outstanding capacitance for flexible Solid-state supercapacitors, *Appl. Surf. Sci.*, 2022, **599**, 154015.
38 N. M. Abbasi, Y. Xiao, L. Zhang, L. Peng, Y. Duo, L. Wang and P. Yin, *et al.*, Heterostructures of titanium-based MXenes in energy conversion and storage devices, *J. Mater. Chem. C*, 2021, **9**(27), 8395–8465.
39 J. Fu, J. Yun, S. Wu, L. Li, L. Yu and K. H. Kim, Architecturally robust graphene-encapsulated MXene Ti_2CT_x@Polyaniline composite for high-performance pouch-type asymmetric supercapacitor, *ACS Appl. Mater. Interfaces*, 2018, **10**(40), 34212–34221.
40 J. Yan, C. E. Ren, K. Maleski, C. B. Hatter, B. Anasori, P. Urbankowski, A. Sarycheva and Y. Gogotsi, Flexible MXene/graphene films for ultrafast supercapacitors with outstanding volumetric capacitance, *Adv. Funct. Mater.*, 2017, **27**(30), 1701264.
41 K. R. G. Lim, M. Shekhirev, B. C. Wyatt, B. Anasori, Y. Gogotsi and Z. Wei Seh, Fundamentals of MXene synthesis, *Nat. Synth.*, 2022, **1**(8), 601–614.
42 V. Natu, R. Pai, M. Sokol, M. Carey, V. Kalra and M. W. Barsoum, 2D $Ti_3C_2T_z$ MXene synthesized by water-free etching of Ti_3AlC_2 in polar organic solvents, *Chem*, 2020, **6**(3), 616–630.
43 Y. Fan, L. Li, Y. Zhang, X. Zhang, D. Geng and W. Hu, Recent advances in growth of transition metal carbides and nitrides (MXenes) crystals, *Adv. Funct. Mater.*, 2022, **32**(16), 2111357.
44 Y.-Z. Zhang, Y. Wang, Q. Jiang, J. K. El-Demellawi, H. Kim and H. N. Alshareef, MXene printing and patterned coating for device applications, *Adv. Mater.*, 2020, **32**(21), 1908486.
45 M. Cao, F. Wang, L. Wang, W. Wu, W. Lv and J. Zhu, Room temperature oxidation of Ti_3C_2 MXene for supercapacitor electrodes, *J. Electrochem. Soc.*, 2017, **164**(14), A3933.

46 R. Ma, X. Zhang, J. Zhuo, L. Cao, Y. Song, Y. Yin, X. Wang, G. Yang and F. Yi, Self-Supporting, Binder-Free, and Flexible $Ti_3C_2T_x$ MXene-Based Supercapacitor Electrode with Improved Electrochemical Performance, *ACS nano*, 2022, **16**(6), 9713–9727.

47 S. Xu, G. Wei, J. Li, Y. Ji, N. Klyui, V. Izotov and W. Han., Binder-free $Ti_3C_2T_x$ MXene electrode film for supercapacitor produced by electrophoretic deposition method, *Chem. Eng. J.*, 2017, **317**, 1026–1036.

48 L. Yu, B. Liu, Y. Wang, F. Yu and J. Ma, Recent progress on MXene-Derived material and its' application in energy and environment, *J. Power Sources*, 2021, **490**, 229250.

49 Y. Huang, Q. Lu, D. Wu, Y. Jiang, Z. Liu, B. Chen, M. Zhu and O. G. Schmidt., Flexible MXene films for batteries and beyond, *Carbon Energy*, 2022, **4**(4), 598–620.

50 R. Syamsai and A. N. Grace, Ta_4C_3 MXene as supercapacitor electrodes, *J. Alloys Compd.*, 2019, **792**, 1230–1238.

51 L. Wang, M. Zhang, B. Yang, J. Tan, X. Ding and W. Li, Recent advances in multidimensional (1D, 2D, and 3D) composite sensors derived from MXene: synthesis, structure, application, and perspective, *Small Methods*, 2021, **5**(7), 2100409.

52 S. Panda, K. Deshmukh, S. K. Khadheer Pasha, J. Theerthagiri, S. Manickam and M. Yong Choi, MXene based emerging materials for supercapacitor applications: recent advances, challenges, and future perspectives, *Coord. Chem. Rev.*, 2022, **462**, 214518.

53 N. K. Chaudhari, H. Jin, B. Kim, D. S. Baek, S. H. Joo and K. Lee, MXene: an emerging two-dimensional material for future energy conversion and storage applications, *J. Mater. Chem. A*, 2017, **5**(47), 24564–24579.

54 T. Kshetri, D. T. Tran, H. T. Le, D. C. Nguyen, H. V. Hoa, N. H. Kim and J. H. Lee, Recent advances in MXene-based nanocomposites for electrochemical energy storage applications, *Prog. Mater. Sci.*, 2021, **117**, 100733.

55 Y. Zhang, L. Wang, N. Zhang and Z. Zhou, Adsorptive environmental applications of MXene nanomaterials: a review, *RSC Adv.*, 2018, **8**(36), 19895–19905.

56 L. L. Zhang and X. S. Zhao., Carbon-based materials as supercapacitor electrodes, *Chem. Soc. Rev.*, 2009, **38**(9), 2520–2531.

57 Z. Yang, J. Tian, Z. Yin, C. Cui, W. Qian and F. Wei, Carbon nanotube-and graphene-based nanomaterials and applications in high-voltage supercapacitor: A review, *Carbon*, 2019, **141**, 467–480.

58 V. Kuzmenko, O. Naboka, M. Haque, H. Staaf, G. Göransson, P. Gatenholm and P. Enoksson, Sustainable carbon nanofibers/nanotubes composites from cellulose as electrodes for supercapacitors, *Energy*, 2015, **90**, 1490–1496.

59 Z. Fan, J. Yan, L. Zhi, Q. Zhang, T. Wei, J. Feng, M. Zhang, W. Qian and F. Wei, A three-dimensional carbon nanotube/graphene sandwich and its application as electrode in supercapacitors, *Adv. Mater.*, 2010, **22**(33), 3723–3728.

60 B. A. Ali, A. H. Biby and N. K. Allam, Fullerene C76: An unexplored superior electrode material with wide operating potential window for high-performance supercapacitors, *ChemElectroChem*, 2020, **7**(7), 1672–1678.

61 C. Ma, L. Wu, M. Dirican, H. Cheng, J. Li, Y. Song, J. Shi and X. Zhang, Carbon black-based porous sub-micron carbon fibers for flexible supercapacitors, *Appl. Surf. Sci.*, 2021, **537**, 147914.

62 T. Jayaraman, A. P. Murthy, V. Elakkiya, S. Chandrasekaran, P. Nithyadharseni, Z. Khan and R. Arumugam Senthil, *et al.*, Recent development on carbon based heterostructures for their applications in energy and environment: a review, *J. Ind. Eng. Chem.*, 2018, **64**, 16–59.

63 Y. Zhong, T. Shi, Y. Huang, S. Cheng, G. Liao and Z. Tang, One-step synthesis of porous carbon derived from starch for all-carbon binder-free high-rate supercapacitor, *Electrochim. Acta*, 2018, **269**, 676–685.

64 D. Wang, G. Fang, T. Xue, J. Ma and G. Geng, A melt route for the synthesis of activated carbon derived from carton box for high performance symmetric supercapacitor applications, *J. Power Sources*, 2016, **307**, 401–409.

65 P. Yu, Y. Liang, H. Dong, H. Hu, S. Liu, L. Peng, M. Zheng, Y. Xiao and Y. Liu, Rational synthesis of highly porous carbon from waste bagasse for advanced supercapacitor application, *ACS Sustainable Chem. Eng.*, 2018, **6**(11), 15325–15332.

66 X. Wang, D. Wu, X. Song, W. Du, X. Zhao and D. Zhang, Review on carbon/polyaniline hybrids: design and synthesis for supercapacitor, *Molecules*, 2019, **24**(12), 2263.

67 S. Saha, P. Samanta, N. C. Murmu and T. Kuila, A review on the heterostructure nanomaterials for supercapacitor application, *J. Energy Storage*, 2018, **17**, 181–202.

68 Z. Yang, J. Tian, Z. Yin, C. Cui, W. Qian and F. Wei, Carbon nanotube-and graphene-based nanomaterials and applications in high-voltage supercapacitor: A review, *Carbon*, 2019, **141**, 467–480.

69 Dieter Vollath, Nanomaterials an introduction to synthesis, properties and application, *Environ. Eng. Manage. J.*, 2008, **7**(6), 865–870.

70 T. Jin, Q. Han, Y. Wang and L. Jiao, 1D nanomaterials: design, synthesis, and applications in sodium–ion batteries, *Small*, 2018, **14**(2), 1703086.

71 Y. Yuan, Z. Chen, H. Yu, X. Zhang, T. Liu, M. Xia, R. Zheng, M. Shui and J. Shu, Heteroatom-doped carbon-based materials for lithium and sodium ion batteries, *Energy Storage Mater.*, 2020, **32**, 65–90.

72 S. S. Siwal, Q. Zhang, N. Devi and V. Kumar Thakur, Carbon-based polymer nanocomposite for high-performance energy storage applications, *Polymers*, 2020, **12**(3), 505.

73 L. Fagiolari and F. Bella, Carbon-based materials for stable, cheaper and large-scale processable perovskite solar cells, *Energy Environ. Sci.*, 2019, **12**(12), 3437–3472.

74 P. Simon and Y. Gogotsi, Materials for electrochemical capacitors, *Nat. Mater.*, 2008, **7**(11), 845–854.

75 L. Yang, W. Zheng, P. Zhang, J. Chen, W. B. Tian, Y. M. Zhang and Z. M. Sun, MXene/CNTs films prepared

by electrophoretic deposition for supercapacitor electrodes, *J. Electroanal. Chem.*, 2018, **830**, 1–6.

76 H. Chen, L. Yu, Z. Lin, Q. Zhu, P. Zhang, N. Qiao and B. Xu, Carbon nanotubes enhance flexible MXene films for high-rate supercapacitors, *J. Mater. Sci.*, 2020, **55**, 1148–1156.

77 T. Zheng, X. Zhang, Y. Li, Y. Zhu, W. Yan, Z. Zhao, L. Zhang, C. Bai and X. Wang, Wet-Spinning of Continuous Hyaluronic-Based MXene/CNTs Hybrid Fibers for Flexible Supercapacitor Applications, *Mater. Lett.*, 2023, 133891.

78 Z. Wang, S. Qin, S. Seyedin, J. Zhang, J. Wang, A. Levitt and N. Li, *et al.*, High-performance biscrolled MXene/carbon nanotube yarn supercapacitors, *Small*, 2018, **14**(37), 1802225.

79 J. W. Park, D. Y. Lee, H. Kim, J. S. Hyeon, M. J. de Andrade, R. H. Baughman and S. Jeong Kim, Highly loaded MXene/carbon nanotube yarn electrodes for improved asymmetric supercapacitor performance, *MRS Commun.*, 2019, **9**(1), 114–121.

80 P. Yan, R. Zhang, J. Jia, C. Wu, A. Zhou, J. Xu and X. Zhang, Enhanced supercapacitive performance of delaminated two-dimensional titanium carbide/carbon nanotube composites in alkaline electrolyte, *J. Power Sources*, 2015, **284**, 38–43.

81 Q. Fu, X. Wang, N. Zhang, J. Wen, L. Li, H. Gao and X. Zhang, Self-assembled $Ti_3C_2T_x$/SCNT composite electrode with improved electrochemical performance for supercapacitor, *J. Colloid Interface Sci.*, 2018, **511**, 128–134.

82 N. Radha, A. Kanakaraj, H. M. Manohar, M. R. Nidhi, D. Mondal, S. K. Nataraj and D. Ghosh., Binder free self-standing high performance supercapacitive electrode based on graphene/titanium carbide composite aerogel, *Appl. Surf. Sci.*, 2019, **481**, 892–899.

83 P. Dutta, A. Sikdar, A. Majumdar, M. Borah, N. Padma, S. Ghosh and U. Narayan Maiti, Graphene aided gelation of MXene with oxidation protected surface for supercapacitor electrodes with excellent gravimetric performance, *Carbon*, 2020, **169**, 225–234.

84 M. Zhang, J. Cao, Y. Wang, J. Song, T. Jiang, Y. Zhang, W. Si, X. Li, B. Meng and G. Wen, Electrolyte-mediated dense integration of graphene-MXene films for high volumetric capacitance flexible supercapacitors, *Nano Res.*, 2021, **14**, 699–706.

85 Q. Yang, Z. Xu, B. Fang, T. Huang, S. Cai, H. Chen, Y. Liu, K. Gopalsamy, W. Gao and C. Gao, MXene/graphene hybrid fibers for high performance flexible supercapacitors, *J. Mater. Chem. A*, 2017, **5**(42), 22113–22119.

86 J. Yan, C. E. Ren, K. Maleski, C. B. Hatter, B. Anasori, P. Urbankowski, A. Sarycheva and Y. Gogotsi, Flexible MXene/graphene films for ultrafast supercapacitors with outstanding volumetric capacitance, *Adv. Funct. Mater.*, 2017, **27**(30), 1701264.

87 L. Yu, L. Hu, B. Anasori, Y.-T. Liu, Q. Zhu, P. Zhang, Y. Gogotsi and B. Xu., MXene-bonded activated carbon as a flexible electrode for high-performance supercapacitors, *ACS Energy Lett.*, 2018, **3**(7), 1597–1603.

88 Y. Tian, C. Yang, Y. Tang, Y. Luo, X. Lou and W. Que, $Ti_3C_2T_x$//AC dual-ions hybrid aqueous supercapacitors with high volumetric energy density, *Chem. Eng. J.*, 2020, **393**, 124790.

89 L. Wang, D. Shao, J. Guo, S. Zhang and Y. Lu, A MXene-coated activated carbon cloth for flexible solid-state supercapacitor, *Energy Technol.*, 2020, **8**(3), 1901003.

90 Y. Li, P. Kamdem and X.-J. Jin., Hierarchical architecture of MXene/PANI hybrid electrode for advanced asymmetric supercapacitors, *J. Alloys Compd.*, 2021, **850**, 156608.

91 K. Li, X. Wang, S. Li, P. Urbankowski, J. Li, Y. Xu and Y. Gogotsi, An ultrafast conducting polymer@MXene positive electrode with high volumetric capacitance for advanced asymmetric supercapacitors, *Small*, 2020, **16**(4), 1906851.

92 C. Zhang, S. Xu, D. Cai, J. Cao, L. Wang and W. Han, Planar supercapacitor with high areal capacitance based on Ti_3C_2/Polypyrrole composite film, *Electrochim. Acta*, 2020, **330**, 135277.

93 L.-G. Gong, X.-X. Qi, K. Yu, J.-Q. Gao, B.-B. Zhou and G.-Y. Yang, Covalent conductive polymer chain and organic ligand ethylenediamine modified MXene-like-$\{AlW_{12}O_{40}\}$ compounds for fully symmetric supercapacitors, electrochemical sensors and photocatalysis mechanisms, *J. Mater. Chem. A*, 2020, **8**(11), 5709–5720.

94 M. Boota and Y. Gogotsi, MXene—conducting polymer asymmetric pseudocapacitors, *Adv. Energy Mater.*, 2019, **9**(7), 1802917.

95 W. Shao, M. Tebyetekerwa, I. Marriam, W. Li, Y. Wu, S. Peng, S. Ramakrishna, S. Yang and M. Zhu, Polyester@MXene nanofibers-based yarn electrodes, *J. Power Sources*, 2018, **396**, 683–690.

96 L. Sun, Q. Fu and C. Pan, Hierarchical porous skin/skeleton-like MXene/biomass derived carbon fibers heterostructure for self-supporting, flexible all solid-state supercapacitors, *J. Hazard. Mater.*, 2021, **410**, 124565.

97 L. Qin, D. Yang, M. Zhang, T. Zhao, Z. Luo and Z.-Z. Yu, Superelastic and ultralight electrospun carbon nanofiber/MXene hybrid aerogels with anisotropic microchannels for pressure sensing and energy storage, *J. Colloid Interface Sci.*, 2021, **589**, 264–274.

98 A. S. Levitt, M. Alhabeb, C. B. Hatter, A. Sarycheva, G. Dion and Y. Gogotsi, Electrospun MXene/carbon nanofibers as supercapacitor electrodes, *J. Mater. Chem. A*, 2019, **7**(1), 269–277.

99 L. Wang, D. Shao, J. Guo, S. Zhang and Y. Lu, A MXene-coated activated carbon cloth for flexible solid-state supercapacitor, *Energy Technol.*, 2020, **8**(3), 1901003.

100 I. Habib, P. Ferrer, S. C. Ray and K. I. Ozoemena, Interrogating the impact of onion-like carbons on the supercapacitive properties of MXene (Ti_2CT_x), *J. Appl. Phys.*, 2019, **126**(13), 134301.

101 L. Li, S. Wu, K. Wu, H. Zhou, Y. Li, M. Guo, L. Qu and Y. Zhou, Carbon dot-regulated 2D MXene films with high volumetric capacitance, *Ind. Eng. Chem. Res.*, 2020, **59**(31), 13969–13978.

102 Q. Fu, X. Wang, N. Zhang, J. Wen, L. Li, H. Gao and X. Zhang, Self-assembled $Ti_3C_2T_x$/SCNT composite electrode with improved electrochemical performance for supercapacitor, *J. Colloid Interface Sci.*, 2018, **511**, 128–134.

103 L. Qin, Q. Tao, L. Liu, J. Jiang, X. Liu, M. Fahlman, L. Hou, J. Rosen and F. Zhang, Flexible Solid-State Asymmetric Supercapacitors with Enhanced Performance Enabled by Free-Standing MXene–Biopolymer Nanocomposites and Hierarchical Graphene–RuOx Paper Electrodes, *Batteries Supercaps*, 2020, **3**(7), 604–610.

104 A. M. Navarro-Suárez, K. Maleski, T. Makaryan, J. Yan, B. Anasori and Y. Gogotsi, 2D titanium carbide/reduced graphene oxide heterostructures for supercapacitor applications, *Batteries Supercaps*, 2018, **1**(1), 33–38.

105 Y. Fang, B. Yang, D. He, H. Li, K. Zhu, L. Wu and K. Ye, *et al.*, Porous and free-standing $Ti_3C_2T_x$-RGO film with ultrahigh gravimetric capacitance for supercapacitors, *Chin. Chem. Lett.*, 2020, **31**(4), 1004–1008.

106 J. S. Seenath and B. P. Biswal, Construction of MXene-Coupled Nitrogen-Doped Porous Carbon Hybrid from a Conjugated Microporous Polymer for High-Performance Supercapacitors, *Adv. Energy Sustainability Res.*, 2021, **2**(3), 2000052.

107 Z. Pan and X. Ji, Facile synthesis of nitrogen and oxygen co-doped C@Ti_3C_2 MXene for high performance symmetric supercapacitors, *J. Power Sources*, 2019, **439**, 227068.

108 L. Yang, W. Zheng, P. Zhang, J. Chen, W. Zhang, W. B. Tian and Z. M. Sun, Freestanding nitrogen-doped d-Ti_3C_2/reduced graphene oxide hybrid films for high performance supercapacitors, *Electrochim. Acta*, 2019, **300**, 349–356.

109 Y. Li, Y. Deng, J. Zhang, Y. Shen, X. Yang and W. Zhang, Synthesis of restacking-free wrinkled $Ti_3C_2T_x$ monolayers by sulfonic acid group grafting and N-doped carbon decoration for enhanced supercapacitor performance, *J. Alloys Compd.*, 2020, **842**, 155985.

110 W. Chen, D. Zhang, K. Yang, M. Luo, P. Yang and X. Zhou, Mxene ($Ti_3C_2T_x$)/cellulose nanofiber/porous carbon film as free-standing electrode for ultrathin and flexible supercapacitors, *Chem. Eng. J.*, 2021, **413**, 127524.

111 X. Gao, X. Du, T. S. Mathis, M. Zhang, X. Wang, J. Shui, Y. Gogotsi and M. Xu, Maximizing ion accessibility in MXene-knotted carbon nanotube composite electrodes for high-rate electrochemical energy storage, *Nat. Commun.*, 2020, **11**(1), 6160.

112 M. Hu, T. Hu, R. Cheng, J. Yang, C. Cui, C. Zhang and X. Wang, MXene-coated silk-derived carbon cloth toward flexible electrode for supercapacitor application, *J. Energy Chem.*, 2018, **27**(1), 161–166.

113 J. Yu, J. Zhou, P. Yao, J. Huang, W. Sun, C. Zhu and J. Xu, A stretchable high performance all-in-one fiber supercapacitor, *J. Power Sources*, 2019, **440**, 227150.

114 H. Li, R. Chen, M. Ali, H. Lee and M. Jae Ko, *In situ* grown MWCNTs/MXenes nanocomposites on carbon cloth for high-performance flexible supercapacitors, *Adv. Funct. Mater.*, 2020, **30**(47), 2002739.

115 X. Li, J. Zhu, L. Wang, W. Wu and Y. Fang, *In situ* growth of carbon nanotubes on two–dimensional titanium carbide for enhanced electrochemical performance, *Electrochim. Acta*, 2017, **258**, 291–301.

116 S. A. Melchior, K. Raju, I. S. Ike, R. M. Erasmus, G. Kabongo, I. Sigalas, S. E. Iyuke and K. I. Ozoemena, High-voltage symmetric supercapacitor based on 2D titanium carbide (MXene, Ti_2CT_x)/carbon nanosphere composites in a neutral aqueous electrolyte, *J. Electrochem. Soc.*, 2018, **165**(3), A501–A511.

117 L. Shen, X. Zhou, X. Zhang, Y. Zhang, Y. Liu, W. Wang, W. Si and X. Dong., Carbon-intercalated $Ti_3C_2T_x$ MXene for high-performance electrochemical energy storage, *J. Mater. Chem. A*, 2018, **6**(46), 23513–23520.

118 X. Zhou, Y. Qin, X. He, Q. Li, J. Sun, Z. Lei and Z.-H. Liu, $Ti_3C_2T_x$ Nanosheets/$Ti_3C_2T_x$ Quantum Dots/RGO (Reduced Graphene Oxide) Fibers for an All-Solid-State Asymmetric Supercapacitor with High Volume Energy Density and Good Flexibility, *ACS Appl. Mater. Interfaces*, 2020, **12**(10), 11833–11842.

119 Y. Kumar, M. Gupta and S. Sharma, Study of pristine and functionalized V2C and Mo2C MXenes as novel electrode material for supercapacitors, *J. Mol. Graphics Modell.*, 2023, **118**, 108366.

120 M. Zhang, D. Jiang, F. Jin, Y. Sun, J. Wang, M. Jiang, J. Cao, B. Zhang and J. Liu., Compression-tolerant supercapacitor based on $NiCo_2O_4$/$Ti_3C_2T_x$ MXene/reduced graphene oxide composite aerogel with insights from density functional theory simulations, *J. Colloid Interface Sci.*, 2023, **636**, 204–215.

121 T. Yuan, Z. Zhang, Q. Liu, X. T. Liu, Y. N. Miao and C. L. Yao, MXene ($Ti_3C_2T_x$)/cellulose nanofiber/polyaniline film as a highly conductive and flexible electrode material for supercapacitors, *Carbohydr. Polym.*, 2023, **304**, 120519.

122 S. Chetana, S. Upadhyay, N. C. Joshi, N. Kumar, P. Choudhary, N. Sharma and V. N. Thakur, A facile supercritical fluid synthesis of cobalt sulfide integrated with MXene and PANI/PEDOT nanocomposites as electrode material for supercapacitor applications, *FlatChem*, 2023, **37**, 100456.

123 O. P. Nanda, A. G. Prince, L. Durai and S. Badhulika, Nickel MXene Nanosheet and Heteroatom Self-Doped Porous Carbon-Based Asymmetric Supercapacitors with Ultrahigh Energy Density, *Energy Fuels*, 2023, **37**(6), 4701–4710.